ELSEVIER

Coordination Chemistry Reviews
151 (1996) 1–40

COORDINATION CHEMISTRY REVIEWS

Coordination chemistry of metallodrugs: insights into biological speciation from NMR spectroscopy[1]

Susan J. Berners-Price [a], Peter J. Sadler [b]

[a] *Faculty of Science and Technology, Griffith University, Nathan, Brisbane, Qld. 4111, Australia*
[b] *Department of Chemistry, Birkbeck College, University of London, Gordon House, 29 Gordon Square, London WC1H 0PP, UK*

Contents

Abstract 1
1. Metallodrugs and diagnostic agents 2
2. Speciation of metallodrugs by NMR 7
   2.1. Scope and Limitations 7
   2.2. Body fluids and cell culture media 9
3. Gold antiarthritic drugs 11
4. Metal phosphine antitumour drugs 12
   4.1. ^{31}P NMR 12
   4.2. ^{31}P–{^{109}Ag} NMR 14
   4.3. Solid state ^{31}P CP-MAS NMR 15
5. Platinum anticancer drugs 19
   5.1. ^{195}Pt NMR 19
   5.2. ^{15}N NMR 20
   5.3. Inverse ^{1}H–{^{15}N} NMR 21
6. Interaction of metallodrugs with blood plasma proteins 29
   6.1. Albumin 30
      6.1.1. N-Terminal Cu(II) and Ni(II) site 30
      6.1.2. Gold binding at Cys34 32
   6.2. Transferrin 32
Acknowledgements 37
References 37

Abstract

There is much current interest in the design of metal compounds as drugs and diagnostic agents and in understanding the molecular mechanisms of action of metallopharmaceuticals

[1] Based on keynote lectures presented at the Third International Symposium on Applied Bioinorganic Chemistry (ISABC-3), Fremantle, Perth, Western Australia, 11–15 December 1994.

SSDI 0010-8545(95)01215-X

already in clinical use. Central to progress in this area is investigation of the speciation of metal compounds, especially in biological media such as cells, body fluids and cell culture media. Modern multinuclear NMR approaches are very powerful for investigation of the thermodynamics and kinetics of reactions of metal compounds with both small and large biomolecules and it is possible to study the coordination chemistry of metallodrugs under physiologically relevant conditions. For example [^{1}H, ^{15}N] inverse detection methods allow studies of intermediates in the pathways of DNA platination by anticancer drugs and the direct detection of sulphur adducts of platinum drugs in urine. Other applications which are discussed include ligand exchange reactions of gold antiarthritic drugs, copper, silver, gold and ruthenium anticancer agents and bismuth antiulcer drugs. Resolution enhancement, specific isotopic labelling of amino acid side-chains and high field NMR studies of metal nuclei provide insight into the uptake and release of metallopharmaceuticals from the blood plasma proteins albumin (66 kDa) and transferrin (80 kDa). The use of ^{31}P cross-polarization magic angle spinning NMR spectroscopy to investigate the structures of bioactive metal phosphine complexes in the solid state is also described.

Keywords: Biological speciation; NMR; Metallodrug

1. Metallodrugs and diagnostic agents

NMR spectroscopy is a powerful method for investigating the speciation of metal complexes in solution and to a lesser extent in the solid state. Understanding both the thermodynamics and kinetics of metal speciation is crucial to the advancement of inorganic molecular pharmacology. The establishment of structure–activity relationships is an important part of the drug design process. The active complex may not be that administered or tested in vitro; it may be transformed by ligand substitution and/or redox reactions before it reaches the target site. In general our understanding of the biological transformations of metallodrugs is very poor compared with that for organic drugs, for which glucuronidation, sulphonation, thiol conjugation, epoxidation, etc. are all well-known metabolic events which can be incorporated into the design process.

Progress is needed on two fronts for both therapeutic and diagnostic agents, first in relation to the metal compounds which are in current clinical use [1,2] and second for novel agents in the discovery and developmental stages. One of the biggest challenges lies in the control of the toxicities of metal compounds and hence in understanding the species which are responsible. The roles played by the intact metal complex itself and either the metal or its ligands separately must be considered [3]. It is notable that some organic pharmaceutical agents may be directed towards metal targets in the body or require metal binding to function (e.g. the anticancer agent bleomycin which requires iron and dioxygen).

A wide variety of metal compounds are already in clinical use; see Table 1. These include mineral supplements containing e.g. transition metals thought to be essential for mammalian life (Cr, Mn, Fe, Co, Ni, Cu, Mo). Widely used too are antacids, many of which are simple inorganic salts of group 1 (sodium bicarbonate), group 2 (magnesium oxide, trisilicate or carbonate) or group 3 (aluminium hydroxide) metals.

Table 1
Metallodrugs and diagnostic agents: biotransformations and targets

Compound	Use	Transformation events	Biological target
Coenzyme vitamin B_{12} Co(I/II/III)	Essential coenzyme	None (nucleotide tail hooks on to enzyme)	Enzymes requiring coenzyme B_{12}, e.g. methylmalonyl CoA-mutase
cis-$[Pt^{II}Cl_2(NH_3)_2]$ Cisplatin	Anticancer drug	Aquation, L-Met adducts, GSH (pumping Pt out of cells), metallothionein	DNA
cis-$[Pt^{II}(CBDCA)(NH_3)_2]$ Carboplatin	Anticancer drug	L-Met adducts, ring opening and release of CBDCA, GSH, metallothionein	DNA
cis, trans, cis-$[Pt^{IV}Cl_2(OAc)_2(NH_3)(C_6H_{11}NH_2)]$	Oral anticancer agent	Reduction, Pt(IV)→Pt(II)	DNA
Na_2Au^I thiomalate Myocrisin	Antiarthritic drug	Thiol exchange, Cys34 albumin, metallothionein, $[Au(CN)_2]^-$, oxidation to Au(III)?	Lysosomes (aurosomes), protein-SH
Et_3PAu^I(tetra-acetylthioglucose)] Auranofin	Oral antiarthritic drug	Phosphine oxidation, Au(I)→Au(III)?	Lysosomes (aurosomes), protein-SH
$[Au^I(Ph_2P(CH_2)_2PPh_2)_2]Cl$	Anticancer agent, antimitochondrial agent	Little, exchange with Cu(I)?	Mitochondria
$[Ag^I(Ph_2P(CH_2)_2PEt_2)_2]NO_3$	Antimitochondrial agent	Phosphine oxidation	Mitochondria
Ag^I sulphadiazine	Antimicrobial agent (burn wounds)	Protein binding (metallothionein?)	DNA?, membranes?, proteins?
Colloidal Bi^{III} citrate	Antiulcer, antimicrobial	GSH?, metallothionein?	Membrane surfaces, *Helicobacter pylori* in ulcers

Table 1 (*continued*)

Compound	Use	Transformation events	Biological target
$Na_2[Fe^{II}(NO)(CN)_5]$	Hypotensive drug (vasodilator)	Release of CN^-, reaction with thiols	Delivery of NO to guanylate cyclase
Li_2CO_3	Manic depression	Widely distributed in body	Enzymes in inositol phosphate pathways
Alkyl $Hg^{II}(OH)$	Diuretic	Thiol exchange reactions?	Membrane pumps?
Phenyl Hg^{II} nitrate	Antimicrobial agent	Thiol exchange, reactions?	Proteins? DNA?
$[Gd^{III}(DTPA)](meglumine)_2$ $[Gd^{III}(DOTA)]^-$	MRI contrast	None	Extracellular water
$^{99m}Tc^{V}$ propyleneamineoxime	Diagnostic radio-imaging (brain)	Ligand exchange?, retained by protonation	Brain
$[^{99m}Tc^{I}(RNC)_6]^+$	Diagnostic radio-imaging (heart)	?	Myocytes (heart)
^{186}Re hydroxyethylidene diphosphonate	Palliative for cancer	Localizes in bone (hydroxyapatite)	Cancer cells
$^{67}Ga^{III}$ citrate	Diagnostic radio-imaging	Ga-transferrin	Tumours and inflammatory lesions
$^{51}Cr^{VI}$ chromate	Radiolabelling cells	Cr(VI)→Cr(III)?	Retained in cells
$Ba^{II}SO_4$	X-Ray contrast agent (GI tract)	None (insoluble)	Passage through GI tract
$Mg^{II}O$	Antacid, laxative	Solubilization and neutralization	Stomach acid
$Mg^{II}SO_4 \cdot 7H_2O$	Laxative	None	Bowel
$Al^{III}(OH)_3$	Antacid, phosphate removal (kidney failure)	Complexation by citrate and transferrin, formation of aluminosilicate	Acid and phosphate in stomach, brain toxic

[Sn^{IV} protoporphyrin $(Cl)_2$]	Treatment of jaundice	None	Inhibits haem oxygenase
Zr^{IV} glycinate, lactate	Antiperspirant	None	Skin
[$V^{IV}(maltol)_2O$]	Insulin mimetic	V(IV)/V(V), ligand exchange?	ATPase enzymes?
[$Sr^{II}(acetate)_2$]	Toothpaste	Ca^{2+} exchange	Apatite (teeth) oral bacteria?
[Zn^{II}(citrate)]	Antiplaque (toothpastes)	Ligand exchange	Oral bacteria
Ph_3Sn^{IV} benzoates $^nBu_2Sn^{IV}$ 2,5-dihydroxybenzoates	Anticancer agent	Hydrolysis?	Unknown, DNA?
[$(C_5H_5)_2Ti^{IV}Cl_2$]	Anticancer agent	Hydrolysis?	DNA
[$Ti^{IV}(bzacac)_2(OEt)_2$] Budotitane	Anticancer agent	Hydrolysis	DNA?
trans-[$Ru^{III}(im)_2Cl_4$]imH	Anticancer agent	Hydrolysis	DNA?
Spirogermanium	Anticancer agent	?	DNA?
Na[Sb^V gluconate]	Antileishmanial	Unknown	Parasites in liver
Fe^{II} succinate and other dietary supplements	Mineral supplement	Various	Circulatory system

Recently interest in bismuth antacids has revived in relation to the treatment of ulcers, since bismuth compounds are toxic to *Helicobacter pylori*, the bacteria which are thought to prevent ulcers from healing. Lithium salts are effective for controlling mood and are used on a large scale (about one in 1500 of the population) for the treatment of manic depression.

Gold as $K[Au(CN)_2]$ was introduced at the turn of this century for the treatment of tuberculosis and was subsequently replaced by gold(I) thiolates, which were later used (about 1930) for the treatment of rheumatoid arthritis. Today several injectable gold(I) thiolates are used clinically (e.g. aurothiomalate, aurothioglucose, aurothiopropanol sulphonate) and also the orally active drug auranofin. It is curious that the transformation of gold(I) into the biscyanide complex appears to be a natural process in the body (see Section 3).

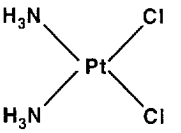

1

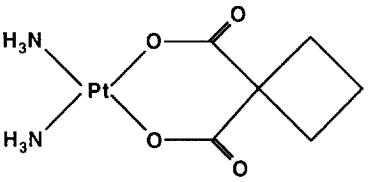

2

The introduction of the platinum(II) complexes cisplatin, *cis*-$[PtCl_2(NH_3)_2]$ (**1**), and carboplatin, *cis*-$[Pt^{II}(CBDCA)(NH_3)_2]$ (**2**) (where CBDCA is 1,1- dicarboxycyclobutane), has dramatically improved the success rate for the treatment of certain types of cancer, notably testicular cancer. A key step in avoiding toxic effects on the kidney is to formulate the drug in saline solution to prevent hydrolysis of the complex. The main target site for platinum is DNA and, specifically, intrastrand cross-links involving guanine and adenine bases. Sulphur ligands such as the amino acid L-methionine and glutathione are also involved in the metabolism of platinum drugs. There is current interest in the development of orally active platinum drugs in complexes which are active against a wider range of types of cancer (e.g. colon cancer) and in complexes which are active against Pt-resistant cancer cells. A Pt(IV) complex *cis,trans,cis*-$[PtCl_2(acetate)_2(NH_3)(cyclohexylamine)]$ has recently entered phase II clinical trials and is probably a pro-drug for its Pt(II) metabolite which lacks axial acetate ligands. Complexes of Ru(III) and Ti(IV) have also entered clinical trials and promise to have a different spectrum of action from platinum drugs [4].

The nitrosyl complex sodium nitroprusside, $Na_2[Fe(CN)_5(NO)]$, which is used in the control of blood flow (vasodilation), is an example of a metal complex which carries a reactive ligand, nitric oxide, to its target site (the enzyme guanylate cyclase).

In the diagnostics field, insoluble barium sulphate has long been used as an X-ray contrast agent for imaging the gastrointestinal tract, but now, for many purposes,

X-ray imaging is being replaced by NMR imaging. NMR contrast agents approved for clinical use include Gd(III) complexes with DTPA (diethylenetriaminepentaacetate) and DOTA (1,4,7,10-tetra(carboxymethyl)-1,4,7,10-tetraazacyclododecane) as ligands. These complexes are both thermodynamically stable and kinetically inert and are excreted from the body largely unchanged.

Radioisotopes ^{99m}Tc and ^{111}In are widely used in radiodiagnostic agents, e.g. for imaging myocardial and cerebral perfusion and monitoring kidney function, depending on the type of ligands and the overall charge on the complex.

The pharmacological activities of these metal compounds will depend on the metal, its ligands or both. An example where the intact metal complex reaches the target site is the cobalt complex vitamin B_{12}, the only cobalt complex which seems to be essential. A recent X-ray structure [5] shows that this coenzyme binds to a fragment of the enzyme methionine synthase between helical and α/β domains. Methylcobalamin bound to the enzyme is intact, although it undergoes a conformational change: the coordinated diemethylbenzimidazole group which is coordinated to cobalt in the free coenzyme is displaced by a His residue and binds in a deep pocket in the protein. The coenzyme is therefore bound to the enzyme in much the same way as haem is bound to myoglobin or haemoglobin. Classical kinetically inert d^3 and d^6 metal complexes such as $[M(phen)_3]^{3+}$ also exhibit their potent neuromuscular blocking activity as intact complexes by binding to acetylcholine esterase, interfering with the function of acetylcholine. The potency depends on the chirality of the complex [6,7], although these compounds have not yet found any use as drugs. However, classical inertness observed in vitro cannot be assumed to prevail in vivo. There is a wide range of reducing agents available in vivo, as well as binding sites on macromolecules which may lower activation energies for substitution reactions, together with a wide range of media of varying dielectric constant (e.g. cell membranes). Also, the pH in vivo is variable: from pH 7.4 in blood plasma, to pH 5.5 in some intracellular compartments (e.g. endosomes, the site of iron release from transferrin), pH 4 in atherosclerotic lesions, down to pH 2 in the stomach, and as high as pH 8 in urine. Some examples of known or possible biotransformations of metallodrugs and diagnostic agents are given in Table 1.

In this article we describe examples of the application of NMR spectroscopy to the speciation of metallopharmaceutical and metallodiagnostic agents in solution and in the solid state, including biofluids and cells and complexation to macromolecular ligands (serum proteins). Because this article is based on lectures given at the Third International Symposium on Applied Bioinorganic Chemistry (ISABC-3), the examples used are taken largely from our own work and we have not attempted to review the field comprehensively.

2. Speciation of metallodrugs by NMR

2.1. Scope and Limitations

Spin-$\frac{1}{2}$ nuclei offer the most potential for studies of metallodrugs. ^{3}H is the most receptive nucleus to NMR detection. It is radioactive, but double-walled glass NMR

tubes offer sufficient protection for NMR experiments. ^{1}H NMR spectroscopy will continue to be the most widely used for investigating ligand behaviour. The sensitivity of ^{1}H detection increases as approximately $B_0^{3/2}$ and so high frequencies (e.g. 600, 750 MHz) offer significant advantages. However the T_1 values of protons in macromolecules may increase with increase in field strength (depending on the rotational correlation time and position of the T_1 minimum) and eventually (above 1 GHz?) relaxation *via* chemical shift anisotropy may become a problem for ^{13}C and ^{15}N just as it is at lower fields for heavier nuclei.

Increasingly, ^{1}H NMR is being used for the inverse detection of other spin-$\frac{1}{2}$ nuclei to which it is coupled, especially ^{13}C and ^{15}N (Section 5.3), although the sensitivity of direct detection of heteronuclei can be enhanced by use of polarization transfer methods such as INEPT and DEPT.

^{31}P with 100% abundance and high sensitivity is invaluable for studies of metal phosphine drugs (Section 4.1) and here also indirect detection of other low γ spin-$\frac{1}{2}$ nuclei (e.g. ^{109}Ag) is possible to gain direct information about the metal coordination sphere. For organotin antitumour compounds there are three spin-$\frac{1}{2}$ isotopes; ^{119}Sn has the highest natural abundance (8.6%) and a receptivity greater than that of ^{13}C (4.44×10^{-3} with respect to ^{1}H) and is most useful for NMR studies. Indirect ^{1}H-$\{^{119}Sn\}$ NMR studies have proved useful in the structural characterization of organotin antitumour compounds by the detection of both long-range and small ^{1}H–^{119}Sn couplings [8].

Only in a few cases is the study of quadrupolar nuclei fruitful for metallodrug work, although the situation may improve with the increasing availability of very high field instruments which offer quite dramatic sharpenings of the central transition of half-integer quadrupolar nuclei [9] (e.g. ^{27}Al, ^{45}Sc, ^{71}Ga; see Section 6.2). Other candidates include ^{25}Mg, ^{43}Ca and ^{67}Zn. ^{63}Cu and ^{65}Cu are both spin $I=\frac{3}{2}$ (abundance 69% and 31% respectively) and of some value in the study of copper phosphine antitumour agents [10]. Although ^{63}Cu has a high abundance, the ^{65}Cu isotope is preferred for NMR studies because it gives narrow lines (smaller quadrupole moment). $^{63/65}Cu-^{31}P$ couplings are resolved only in highly symmetrical $[Cu(PR_3)_4]^+$ complexes; in most cases lines are broadened by the dominant quadrupolar relaxation mechanism. A particular problem lies with the group 15 elements As, Sb and Bi, which are of much interest in pharmacology [11]. All possess only quadrupolar isotopes with large quadrupole moments: ^{75}As (100%, $I=\frac{3}{2}$), ^{121}Sb (57.25%, $I=\frac{5}{2}$), ^{123}Sb (42.75%, $I=\frac{7}{2}$), ^{209}Bi (100%, $I=\frac{9}{2}$). Only in highly symmetrical complexes do these nuclei give rise to reasonably sharp resonances.

Progress in the design of drugs based on group 15 elements is being greatly held up through lack of a suitable probe of the metal itself, although some studies can be made via ligand nuclei. For example, the binding of citrate to Bi(III) in antiulcer complexes such as CBS (colloidal bismuth citrate) [12,13] and rantidine bismuth citrate [14] has been studied by ^{1}H and ^{13}C NMR spectroscopy. Citrate is a good bridging ligand and polymeric species are formed in solution. Second-coordination-sphere interactions between coordinated citrate and ranitidine can be detected by NMR. The strong, short Bi(III) alkoxide bond is a notable feature of these complexes. Little is known about the preference of Bi(III) for different ligand types or the

kinetics of ligand exchange reactions and these are currently being studied by NMR methods. The rate of uptake of Bi(III) into red blood cells and complexation with intracellular glutathione, as determined by ^{1}H NMR, is relatively slow (hours) [15].

Metal compounds that contain unpaired electrons in general give rise to broadenings and shifts of ligand NMR resonances, broadenings being the most severe when the electron spin relaxation time is long (e.g. Mn(II), Gd(III)), an effect which is made use of in the design of contrast agents for magnetic resonance imaging. Encapsulation of Gd(III) with a strongly binding ligand such as DTPA or DOTA renders the complex non-toxic (excreted intact) and still allows H_2O molecules to bind, since Gd(III) can adopt high coordination numbers of nine or 10, thereby affecting the relaxation times of water in tissues and so giving rise to the required contrast [16].

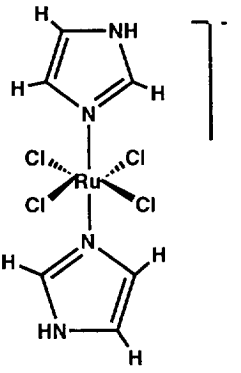

(3)

Octahedral Ru(III) (low spin d^5, one unpaired electron) has a relatively short electron spin relaxation time and acquisition of EPR spectra requires the use of very low temperatures (e.g. 10 K). Paramagnetically shifted ^{1}H NMR resonances are readily detected in ^{1}H NMR spectra of Ru(III) complexes and can be used to determined the rate of hydrolysis of the anticancer complex $[RuCl_4(Im)_2]^-$ (**3**) (Im means imidazole); see Fig. 1 [17]. This occurs on a similar time scale ($t_{1/2}=3.4$ h at 37 °C) to the hydrolysis of cisplatin ($t_{1/2}=2.6$ h).

2.2. Body fluids and cell culture media

Both body fluids and cell culture media are complicated, often heterogeneous media. For example, blood plasma contains fat particles (lipoproteins) which contain triacylglycerols, phospholipids and cholesterol, large proteins (e.g. immunoglobulins, albumin and transferrin) as well as many small molecules and ions. When metal compounds are tested for activity in vitro using cells in culture, they may be chemically transformed via ligand substitution or redox reactions in the cell culture

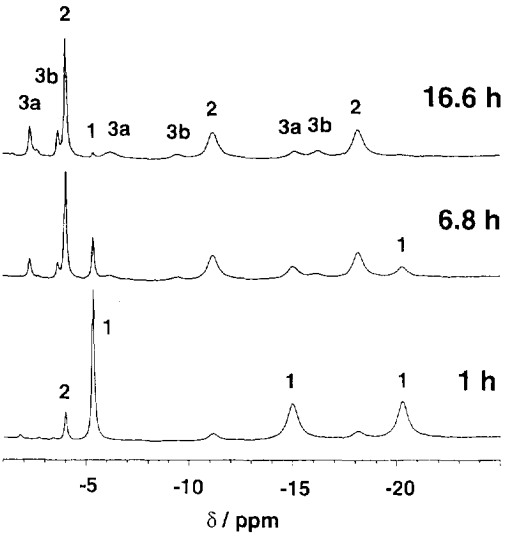

Fig. 1. Hydrolysis of the anticancer complex $[RuCl_4(Im)_2]Im$ (3) as seen in 270 MHz ^1H NMR spectra at various times after dissolution in D_2O at 37 °C (body temperature). Paramagnetically shifted peaks (Ru(III), low spin d^5) for the initial complex 1 are replaced by peaks assignable to the mono- (2) and di-aqua complexes (3a and 3b). The shifts are predominantly dipolar in origin. (Adapted from Ref. [17].)

medium (a medium which often resembles blood plasma in composition). Although model reactions can be set up to investigate this, direct studies of the coordination chemistry of metal complexes in intact biofluids are needed.

For example, when cisplatin is incubated with Dulbecco's cell culture medium, the singlet for the S-methyl of the L-methionine in the medium disappears and a new peak characteristic of Pt-bound L-Met appears [18].

^1H NMR experiments of plasma show that reactions of copper complexes in plasma involve a range of low molecular mass ligands as well as transfer of Cu(II) into the N-terminal site of albumin [19]. When the copper donor is the EDTA complex, then transfer on to albumin is relatively slow, with a half-life of 26 min at 21 °C. Metal binding to proteins in blood plasma can be accompanied by changes in the binding of other molecules. For example, the complex $[Cu^{II}_2(DIPS)_4]$ (DIPS ≡ diisopropylsalicylate) displaces lactate from protein binding. The DIPS ligands are readily displaced by components of urine. ^1H NMR spectra suggest that formate, citrate and histidine are involved in competitive Cu(II) binding (paramagnetic broadening of peaks) [19].

Direct binding of Al^{3+} to citrate in blood plasma has been detected by ^1H NMR spectroscopy at concentrations as low as 50 μM and reversal of binding by addition of desferrioxamine [20]. From citrate, Al(III) is transferred to transferrin and via transferrin receptors into the brain where it is toxic. Al(III) is apparently readily removed from the body if the kidneys are functioning normally, presumably because Al(III) citrate complexes are then readily filtered out of the blood.

3. Gold antiarthritic drugs

The gold(I) complexes in clinical use for the treatment of rheumatoid arthritis are linear and two-coordinate. The orally active complex auranofin (**4**) (Et_3PAuSR, where SR means tetraacetylthioglucose) is a monomer which undergoes facile deacetylation in the acidic conditions of the stomach. The hydrolysis can be followed by ^1H NMR spectroscopy with the release of acetic acid [21]. The injectable gold(I) thiolate complexes such as aurothiomalate (**5**) are polymers. Although aurothiomalate has a nominal 1:1 stoichiometry, it usually contains a 10–15 mol% excess of thiol over gold and is probably composed of a mixture of cyclic hexamers and linear oligomers. The structures of these polymers are very sensitive to the ionic strength and pH of the solutions.

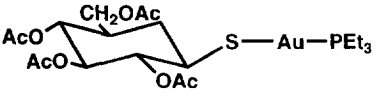

Auranofin

(4)

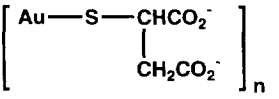

Aurothiomalate

(5)

These linear gold(I) drugs undergo facile ligand exchange reactions and ^{13}C NMR studies show that thiols with the lowest pK_a values bind the most strongly to Au(I) [22]. It is therefore perhaps not surprising that gold becomes widely distributed in the body after drug administration, a major site for gold transport being Cys34 of the blood protein albumin, which has a low pK_a (about 5; Section 6.1.2). For gold(I) phosphine drugs (e.g. auranofin) ^{31}P NMR is useful for probing these ligand exchange reactions in biofluids, cells and proteins [21–25]. The ^{31}P shift of the phosphine is sensitive to the nature of the coordinated ligand X and release of PEt_3 can be monitored by observation of a peak for Et_3PO. In R_3P–Au–SR complexes the ^{31}P shift is dependent on the pK_a of the thiolate (SR) [24].

Cyanide appears to play a key role in the metabolism of gold drugs. Arthritic patients treated with either aurothiomalate or auranofin excrete $[Au(CN)_2]^-$ in their urine [26,27]. Surprisingly, cyanide seems to be a natural metabolite in the body, being produced by the oxidation of thiocyanate by the enzyme myeloperoxidase in the white blood cells called polymorphonuclear leukocytes (PMNs). The level of $[Au(CN)_2]^-$ is higher for smokers than for non-smokers on account of the inhalation

of HCN in cigarette smoke. In the liver this HCN is metabolized to SCN^- which circulates in blood plasma and can be reconverted back to cyanide by PMNs. The red blood cell level of gold in patients treated with aurothiomalate is also higher for smokers and can be accounted for by the ease with which $[Au(CN)_2]^-$ is taken up by cells compared with polymeric aurothiomalate [28]. Reactions of aurothiomalate with cyanide can be followed readily by ^1H or ^{13}C NMR spectroscopy (using ^{13}C-enriched cyanide) [29]. These show that the mixed ligand complex $[Au(Stm)(CN)]^-$, where Stm is S-bound thiomalate, readily forms as an intermediate at cyanide/aurothiomalate ratios less than 2 and this complex gives rise to the bisthiomalato complex by disproportionation. At higher ratios $[Au(CN)_2]^-$ is the major product. Since $[Au(CN)_2]^-$ inhibits the oxidative burst of PMNs (these cells are usually found in high numbers in synovial fluid in the joints of rheumatoid patients) and itself can act as an antiarthritic agent and inhibit proliferation of lymphocytes, it may be a key gold species in understanding the antiarthritic activity of gold complexes.

4. Metal phosphine antitumour drugs

4.1. ^{31}P NMR

Auranofin and a large number of other linear Au(I) phosphine complexes are potently cytotoxic to tumour cells in culture [25]. However, in vivo auranofin exhibits modest antitumour activity, against only intraperitoneal P388 leukaemia in mice, and then only when administered intraperitoneally (i.e. the drug comes into direct contact with the tumour cells). In contrast, bis-chelated Au(I) phosphine complexes related to $[Au(dppe)_2]^+$ (**6**) (where dppe ≡ 1,2-bis(diphenylphosphino)-ethane) are active against a spectrum of tumour models in mice [30]. This difference is likely to be related to the lower thiol reactivity of the tetrahedral complexes, which can undergo ligand exchange reactions only by chelate ring opening. ^{31}P NMR studies have shown that $[Au(dppe)_2]^+$ (unlike auranofin) remains essentially intact in human plasma [31] and does not react significantly with glutathione or albumin.

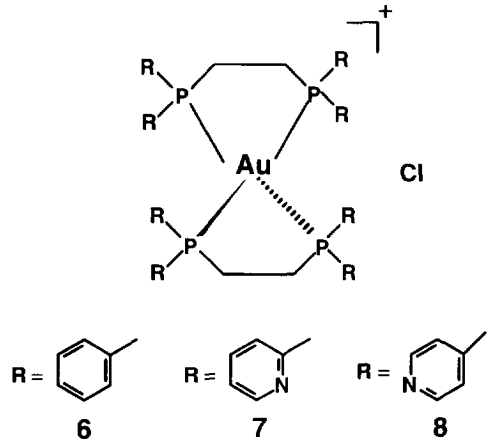

For complexes of the type $[Au(R_2P(CH_2)_nPR'_2)_2]^+$, highest activity was found with $R \equiv R' \equiv Ph$ and $n=2$, 3 or *cis*-CH=CH. The free diphosphine ligand (dppe) showed a similar spectrum and degree of antitumour activity to $[Au(dppe)_2]Cl$ in mice, suggesting that part of the action of Au(I) is to protect the ligand from oxidation reactions before it reaches the target site. Activity is retained when Au(I) is substituted by Ag(I) and Cu(I) and these have a similar kinetic lability of the M—P bonds. If the phenyl substituents on the phosphine are replaced by other substituents, antitumour activity is generally reduced or lost altogether [30]. This may be related to the higher reactivity of alkyl- compared with aryl-phosphines towards disulphide bonds. For example, $[Au(eppe)_2]^+$ (R is Ph; R′ is Et) was shown by ^{31}P NMR to slowly cleave disulphide bonds in albumin with release of the phosphine oxide [32]. Similarly, the analogous Ag(I) complex $[Ag(eppe)_2]NO_3$, which exhibits potent antimitochondrial activity in yeast [33], is stable in the presence of glutathione but reacts rapidly with albumin with release of $Et_2P(O)(CH_2)_2P(O)Ph_2$.

Recent ^{31}P NMR studies of tetrahedral bisphosphine Au(I) complexes with pyridyl substituents (R and R′ are 2-pyridyl (**7**), 4-pyridyl (**8**)) have shown that these are stable for at least 30 h when incubated in blood plasma at 37 °C [34]. However, whereas the 2-pyridyl complex shows potent antitumour activity against P388 leukemia in mice, the 4-pyridyl analogue is inactive [32]. The contrasting activities may be related to differences in their uptake into cells. Whereas the 2-pyridyl complex readily partitions between plasma and red cells (Fig. 2), the 4-pyridyl complex, which

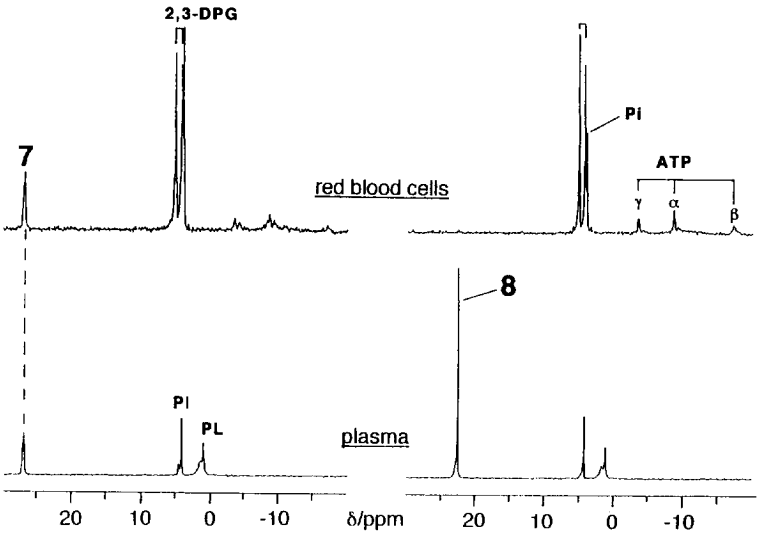

Fig. 2. ^{31}P NMR spectra of the separated plasma and red blood cells from whole human blood which had been incubated for 5 h at 25 °C with the Au(I) bispyridylphosphine complexes **7** (R ≡ 2-pyridyl; left) and **8** (R ≡ 4-pyridyl; right) at a concentration of 1 mM. Whereas the 2-pyridyl complex (**7**) partitions between the plasma and the red blood cells, the 4-pyridyl complex (**8**) is retained in the plasma fraction. PL, phospholipid; 2,3-DPG, 2,3-diphosphoglycerate; Pi, inorganic phosphate.

has a higher water solubility, is retained in the blood plasma fraction. Notable also for the 2-pyridyl complex is the observation of a ^{31}P signal for the intact complex inside the cell. In red cells incubated with $[Au(dppe)_2]Cl$, the ^{31}P signal for the tetrahedral complex was broadened beyond detection and appeared only after disruption of the membrane with sodium dodecyl sulphate [35]. This indicates that the 2-pyridyl complex less readily partitions into lipophilic compartments (e.g. lipoproteins, membranes), consistent with its higher water solubility.

Bridged linear digold(I) bisphosphine complexes XAu(dppe)AuX (where X is, e.g., Cl, SGlu) are also cytotoxic in vitro and exhibit in vivo anticancer activity against a wider range of tumours compared with auranofin [30]. ^{31}P NMR studies show that thiols induce conversion of the linear complexes into the tetrahedral complex $[Au(dppe)_2]^+$ and this reaction also occurs in blood plasma [36]. The cellular pharmacology and profile of antitumour activity of GluSAu(dppe)AuSG are similar to those of $[Au(dppe)_2]^+$, which is consistent with the ring-closed product being the major metabolite of the bridged digold complex in vivo and also with the cytotoxic mechanism depending on the selective uptake of lipophilic cationic species into mitochondria.

4.2. ^{31}P–$\{^{109}Ag\}$ NMR

For Ag(I) phosphine antitumour complexes the occurrence of the two spin-$\frac{1}{2}$ isotopes ^{109}Ag and ^{107}Ag with high natural abundance (48.2% and 51.8% respectively) provides an additional useful tool for NMR studies. The one-bond $^{107/109}Ag-^{31}P$ coupling constants provide information about the Ag coordination sphere. For tetrahedral $[Ag(P-P)_2]X$ complexes the $^1J(^{31}P-^{109}Ag)$ coupling constants are usually in the range 230–290 Hz, with $^1J(^{107}Ag-^{31}P)$ smaller by a factor of 0.869 ($\gamma^{107}Ag/\gamma^{109}Ag$). These couplings are generally resolved in the ^{31}P NMR spectra at ambient temperature, showing greatly enhanced kinetic stabilities with respect to Ag(I) complexes of monodentate phosphines [37].

The low receptivities of the ^{109}Ag and ^{107}Ag isotopes (0.28 and 0.20 relative to ^{13}C) and very long spin–lattice relaxation times (e.g. 1115 s for $AgNO_3$ in D_2O) limit their usefulness for direct NMR studies. However, indirect $^{31}P-\{^{109}Ag\}$ NMR methods have been used to study the coordination chemistry of silver(I) diphosphine antitumour complexes [38,39]. The experiments require a triple-resonance $^{31}P/^1H/X$ probe tunable to low frequencies. For example, we have used $^{31}P-\{^{109}Ag\}$ NMR experiments to follow the unusual solution chemistry of the 1:2 Ag(I) complex of 1,2-bis(di(2-pyridyl)phosphino)ethane (2-dpype) [39]. This antitumour complex exists in solution as a mixture of the monomeric bis-chelated Ag(I) complex $[Ag(2\text{-dpype})_2]^+$, dimeric $[Ag(2\text{-dpype})_2]_2^{2+}$ and trimeric $[Ag(2\text{-dpype})_2]_3^{3+}$ (Scheme 1), which contain both bridging and chelated 2-dpype ligands coordinated by the P atoms. $^{109}Ag-^{31}P$ 2D spectra confirmed the existence of the dimeric and trimeric species by correlation of the ^{31}P and ^{109}Ag NMR shifts.

At a concentration of 1 mM in blood plasma at 37 °C, ^{31}P NMR signals assignable to both the monomeric and dimeric species were observed (Fig. 3), suggesting that

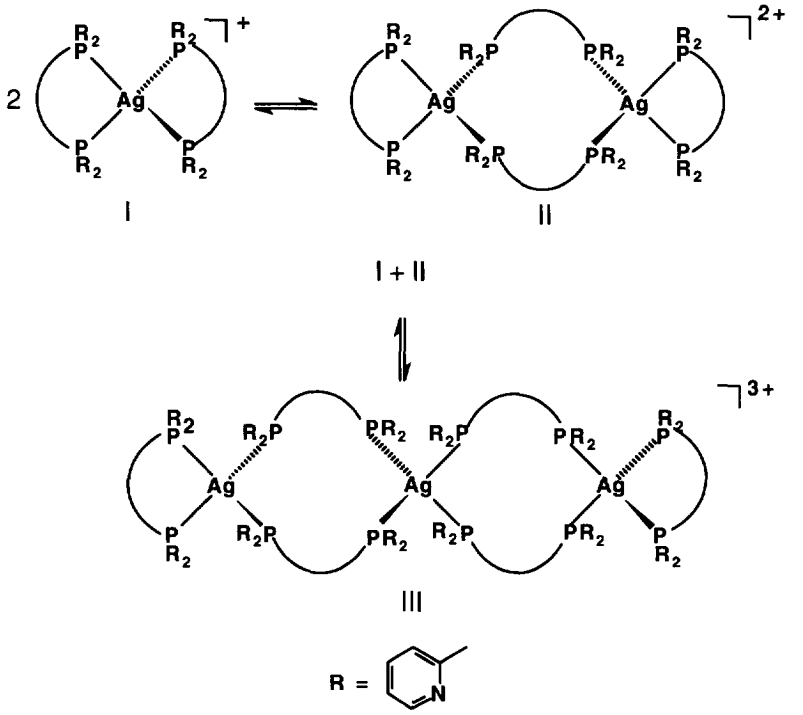

Scheme 1

these equilibria must be taken into account when considering the likely speciation of the complexes in vivo.

4.3. Solid state ^{31}P CP-MAS NMR

^{31}P cross-polarization magic angle spinning (CP-MAS) NMR provides a useful method for studying the relationship between structures characterized in the solid state by X-ray crystallography and those observed in solution by ^{31}P NMR. Crystallographic data need to be interpreted with caution, since a crystal structure (obtained from a single crystal) may not accurately represent the solid state structure of a complex, which could exist as a mixture of several forms. For example, X-ray structures of 1:2 Cu(I) complexes of $Me_2P(CH_2)_2PMe_2$ (dmpe) reveal the existence of both a bis-chelated monomeric complex $[Cu(dmpe)_2]^+$ [40] and a binuclear complex $[Cu(dmpe)_2]_2^{2+}$ [41], with both bridging and chelated dmpe ligands. ^{31}P and ^{63}Cu NMR data were consistent with either the mono- or dimeric form in solution [41]. ^{31}P CP-MAS spectra can confirm whether a complex exists in a unique form in the solid state, so that if more than one species is observed in ^{31}P NMR solution spectra, it is possible to deduce whether the complex undergoes dissociation in solution.

The use of solid state ^{31}P NMR techniques to investigate the coordination chemis-

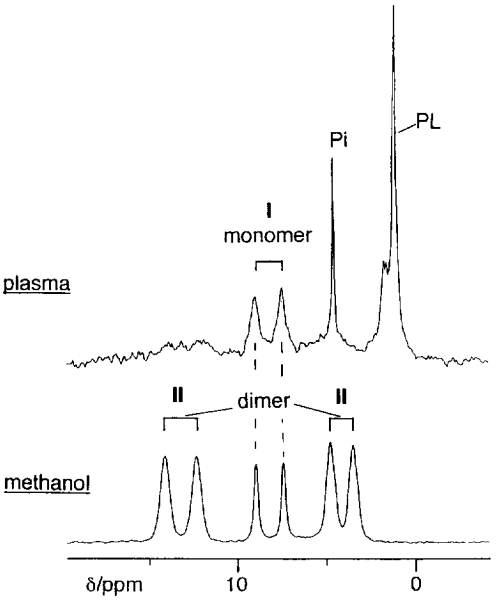

Fig. 3. ^{31}P NMR spectra at 37 °C of the 1:2 Ag(I) complex of 1,2-bis(di(2-pyridyl)phosphino)ethane (2-dpype) in human plasma (top) and methanol (bottom), showing peaks for both monomeric $[Ag(dpype)_2]^+$ and dimeric $[Ag(dpype)_2]_2^{2+}$ (Scheme 1) [39]. PL, phospholipid; Pi, inorganic phosphate.

try of metal phosphine complexes has been reviewed recently [42]. In solution, rapid isotropic motion averages dipolar splittings and the chemical shift anisotropy (CSA) to zero, allowing observation of sharp lines at the isotropic chemical shift. In the solid state, resonances are often broad owing to the existence of non-averaged dipole–dipole and shielding anisotropy interactions. Since both the dipolar coupling and the CSA contain an angular dependence of the form $3\cos^2\theta$-1, spinning a sample at an angle of 54°44′ (the magic angle) with respect to the applied magnetic field (B_0) achieves line narrowing, because then $3\cos^2\theta-1=0$. At spinning speeds below the CSA linewidth a set of sharp lines is observed, spaced at the rotation frequency and centred on the isotropic chemical shift. The pattern of the spinning sidebands can be analysed to extract the principal values of the chemical shift tensor. Alternatively, for complicated spectra it may be preferable to increase the spinning speed to remove all the effects of the CSA, since the spinning sidebands can make spectral interpretation difficult. Typically spinning speeds of the order 3–5 kHz are used. For metal phosphine complexes the dipolar interaction from dipolar coupling to protons is too large for MAS alone to generate usefully sharpened lines and high power dipolar decoupling is also employed. In the CP-MAS experiment, in addition to high power ^1H decoupling and magic angle spinning, magnetization transfer from ^1H to ^{31}P under cross-polarization conditions improves the sensitivity of ^{31}P and also overcomes the problems of the long longitudinal relaxation times (T_1) for dilute ^{31}P spins.

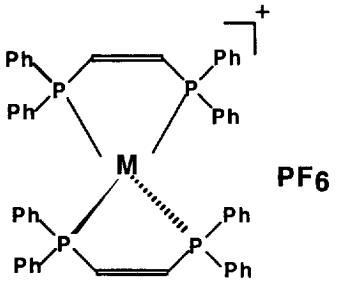

M = Cu(I) M = Au(I)

9 **10**

Correlation of ^{31}P CP-MAS and ^{31}P solution NMR spectra of the 1:2 Cu(I) complex of *cis*-$Ph_2PCH{=}CHPPh_2$ (dppey) confirmed that this antitumour complex exists as the bis-chelated monomeric complex $[Cu(dppey)_2]PF_6$ (**9**) in the solid state and in solution [43]. The ^{31}P CP-MAS spectrum (Fig. 4A) consists of four broad, equally spaced bands with $J(Cu–P) \approx 820$ Hz, interpreted as four closely overlapped quartets for each of the phosphorus atoms which exist in similar chemical environments. Magic angle spinning is only effective in averaging dipolar and indirect coupling in first-order situations when the coupling energy is much smaller than the Zeeman energy. For quadrupolar nuclei the quadrupolar coupling energies are frequently comparable in magnitude with the Zeeman energies and second-order effects produce distortions in band shapes due to terms in the Hamiltonian involving geometrical dependences other than $3\cos^2\theta$-1. Several authors have discussed the interpretation of MAS spectra of spin $I = \frac{1}{2}$ ^{31}P nuclei coupled to quadrupolar spin $I = 3/2$ ^{63}Cu and ^{65}Cu nuclei. Menger and Veeman [44] reported a calculation of the line position in terms of the copper nuclear Zeeman interaction (Z), the copper nuclear quadrupolar coupling constant (χ), the indirect phosphorus spin–spin coupling constant (J) and the ^{31}P–^{63}Cu dipolar coupling constant (D). The appearance of the spectrum depends on the dimensionless parameter $K = \chi/4Z$ and the ratio $R = D/J$ (usually in the range 0.5–1.0 for copper phosphine complexes). For $[Cu(dppey)_2]PF_6$ minimal distortion of the quartet spacings was observed (Fig. 4A), indicating that the quadrupolar effects are only very small. This suggested a small value for χ, consistent with the high symmetry of the CuP_4 core observed in the X-ray structure. ^{31}P–$^{65/63}Cu$ spin–spin couplings were not resolved in the solution ^{31}P NMR spectrum (Fig. 4B), and since the ^{31}P CP-MAS data indicated a small copper nuclear quadrupolar coupling constant (χ), the relatively fast rate of quadrupolar relaxation was attributed to a relatively long correlation time for molecular reorientation (τ_c) due to the presence of the bulky phenyl substituents.

The crystal structure of the analogous Au(I) complex $[Au(dppey)_2]PF_6$ (**10**) showed it to be isomorphous with the Cu(I) complex. ^{31}P CP-MAS spectra (Fig. 4C) revealed splitting of the phosphorus signal into a quartet, ascribed to Au–P spin–spin coupling effects with $J(Au–P) \approx 200$ Hz. As for the Cu(I) complex, minimal distortion of the quartet spacings indicated an unusually small ^{197}Au quadrupolar coupling

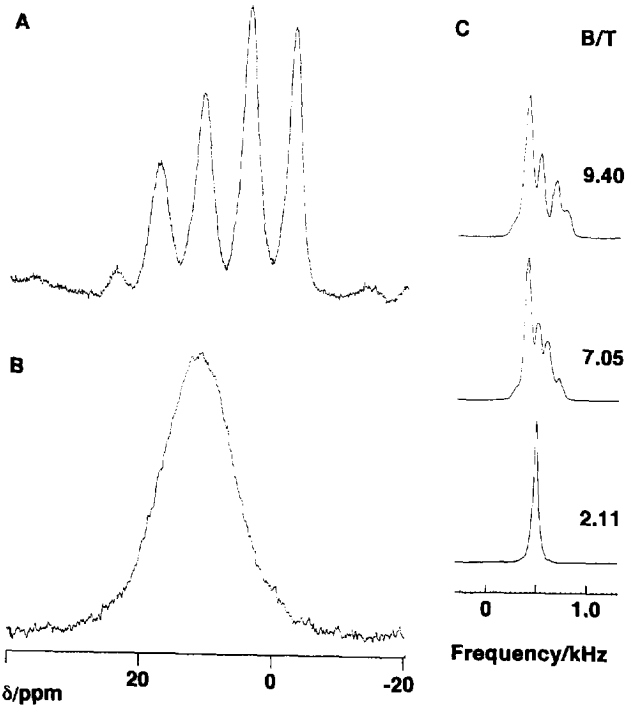

Fig. 4. (A) ^{31}P CP-MAS and (B) solution (CH_2Cl_2, 298 K) ^{31}P NMR spectra of the antitumour complex $[Cu(dppey)_2]PF_6$ (**9**). The lack of distortion in the quartet spacings in (A) is indicative of minimal quadrupolar interaction with the copper nucleus and a small copper quadrupole coupling constant (see text). (C) ^{31}P CP-MAS spectra of the analogous Au(I) complex $[Au(dppey)_2]Cl$ at magnetic field strengths of 2.11, 7.05 and 9.40 T. At the higher field strengths the signal resolves into a quartet with line separations of about 200 Hz, interpreted as indirect spin–spin coupling with the ^{197}Au nucleus. The observation of ^{31}P–^{197}Au coupling is extremely unusual for Au(I) phosphine complexes and suggests a very small ^{197}Au quadrupole coupling constant, consistent with the high symmetry of the AuP_4 coordination sphere observed in the X-ray crystal structure. (Adapted from Ref. [43].)

constant, consistent with the high symmetry of the AuP_4 core. ^{197}Au–^{31}P splittings were not resolved in solution ^{31}P spectra (and have never been observed for an Au(I) phosphine complex), but the similarity of the solution and solid-state ^{31}P chemical shifts indicated that the bis-chelated cation was also stable in solution.

For Ag(I) diphosphine antitumour complexes in particular, the anion may compete for coordination to the metal ion and here it is of particular importance to investigate the relationship between structures that exist in the solid state and in solution. For complexes of the type $Ag(dppp)_2X$ (where dppp is $Ph_2P(CH_2)_3PPh_2$ and X is Cl, Br, I, CN), ^{31}P CP-MAS NMR spectra showed the existence in the solid state of only structures of the type AgP_3X, consistent with the X-ray crystal structures which showed coordinated anion (X) and both chelated and monodentate dppp ligands. In solution the complexes exist in equilibria with other species, including the bis-chelated complex $[Ag(dppp)_2]X$, with the predominant species being dependent on the nature of X [45]. Since the antitumour properties of metal diphosphine complexes

may be related to the selective uptake of lipophilic cations into mitochondria, studies of this type are of fundamental importance to a meaningful interpretation of structure–activity relationships to establish whether the bis-chelated cationic species $[Ag(dppp)_2]^+$ will be the major species present in vivo.

5. Platinum anticancer drugs

5.1. ^{195}Pt NMR

^{195}Pt is a reasonably sensitive nucleus for NMR detection, having a natural abundance of 33.8% and a receptivity relative to ^1H of 3.4×10^{-3}. The limit of detection is about 10 mM. With enrichment of ^{195}Pt, lower concentrations can be detected. Bancroft et al. have studied DNA platination at millimolar levels in this way and have detected both monofunctional and bifunctional guanine adducts [46]. They used ammines containing natural abundance nitrogen (i.e. 99.6% ^{14}N, $I=1$) in their samples and so the ^{195}Pt resonances were broadened by the quadrupolar effects of ^{14}N from both the ammine and the guanine ligands. The shortening of the ^{195}Pt relaxation times by such quadrupolar effects of ^{14}N has the beneficial effect of allowing rapid pulsing without saturation effects. ^{195}Pt–^{14}N couplings in ^{195}Pt NMR spectra are usually better resolved at higher temperatures, because the quadrupolar relaxation rate of ^{14}N decreases (decrease in correlation time).

The ^{195}Pt chemical shift range is large, about 15 000 ppm, and often allows ready differentiation between Pt(II) and Pt(IV), which tend to have chemical shifts at the high field and low field ends of the range respectively. Some caution is required in searching for peaks, because the shifts of Pt(IV) halides alone span 12 000 ppm! Also, there are usually ^{195}Pt chemical shift differences between geometrical isomers and diastereomers. The example of the cisplatin metabolite $[Pt(L\text{-}Met)_2]$ (see Section 5.3) is shown in Fig. 5. Even isotopomers are distinguishable: the ^{195}Pt isotope shift difference for Pt–^{35}Cl and Pt–^{37}Cl is 0.17 ppm and for Pt–^{79}Br and Pt–^{80}Br it is 0.03 ppm [47]. Therefore in principle it is possible to count the number of Cl and Br ligands bonded to Pt via the isotope splitting pattern. For $PtCl_6^{2-}$, for example, a 0.51 : 1.0 : 0.82 : 0.35 : 0.09 : 0.01 : 0.0006 septet is obtained. In practice these isotope shifts are difficult to resolve because of line broadening, which is usually due either to relaxation mechanisms or to poor temperature control of the sample. The latter is a problem because of the strong temperature dependence of ^{195}Pt NMR resonances (up to 1 ppm K^{-1}).

Even in the absence of ^{14}N ligands, ^{195}Pt resonances can be very broad owing to chemical shift anisotropy (CSA) relaxation, which can be the dominant relaxation mechanism for platinum complexes at high magnetic field strength. Similarly, ^{195}Pt satellites in ^{15}N and ^1H spectra of Pt(II) complexes are often broadened beyond detection owing to CSA relaxation of ^{195}Pt [48]. The linewidths of ^{195}Pt satellites of ^1H NMR resonances are dependent on the spin–lattice relaxation time of ^{195}Pt:

$$\Delta\nu_{\frac{1}{2}}(H) = [\pi T_2^*(H)]^{-1} + [2\pi T_1(Pt)]^{-1}$$

where $[\pi T_2^*(H)]^{-1}$ is the natural linewidth plus contributions from magnetic inhomo-

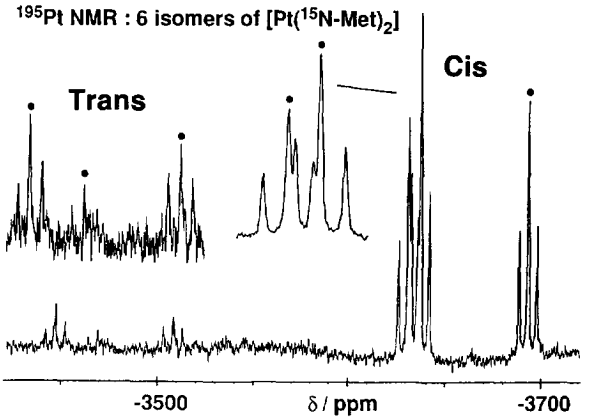

Fig. 5. ^{195}Pt NMR spectrum of [Pt(L-^{15}N-Met)$_2$], a metabolite of the anticancer drug cisplatin, showing three sets of triplets for each of the *cis* and *trans* isomers (Scheme 2). The three diastereomers for each geometrical isomer arise from slow inversion (on the NMR time scale) of chiral coordinated sulphur. (Adapted from Ref. [60].)

geneity broadening (measurable from the linewidth of the centre peak). The contribution to ^{195}Pt T_1 relaxation from CSA is given by

$$[T_1(\mathrm{Pt})]^{-1}(\mathrm{CSA}) = \tfrac{6}{7}[T_2(\mathrm{Pt})]^{-1}(\mathrm{CSA}) = \tfrac{2}{15} \times \gamma_{\mathrm{Pt}}^2 \times B_0^2 \times \Delta\sigma^2 \times \tau_c$$

In general, ^{195}Pt satellites (and ^{195}Pt resonances) are sharper in Pt(IV) complexes which are six coordinate and hence more symmetrical (smaller anisotropy $\Delta\sigma$) and are broader at higher fields of measurement (B_0) and in larger molecules (longer correlation time τ_c).

5.2. ^{15}N NMR

^{15}N NMR chemical shifts and $^1J(^{195}\mathrm{Pt}–^{15}\mathrm{N})$ coupling constants (when resolved) are both sensitive to the nature of the trans ligand in Pt ammine and amine complexes and provide a powerful method for identifying the ligands in the coordination spheres of both Pt(II) and Pt(IV) complexes. Typical shift ranges are shown in Fig. 6. For Pt^{II}–NH_3 complexes the $^1J(^{195}\mathrm{Pt}–^{15}\mathrm{N})$ coupling constants exhibit the following dependence on the trans ligand:

Trans ligand	$^1J(^{195}\mathrm{Pt}–^{15}\mathrm{N})$	Trans ligand	$^1J(^{195}\mathrm{Pt}–^{15}\mathrm{N})$
H_2O	390	Cl^-	310
RCO_2^-	360	NH_3	285
OH^-	340	S(Met)	265

For Pt(IV) they are smaller by a factor of about 1.5 (in theory based on the change in hybridization from dsp^2 to d^2sp^3) to 1.2 (in practice) and are $1.4 \times (\gamma^{15}\mathrm{N}/\gamma^{14}\mathrm{N})$ larger than $^1J(^{195}\mathrm{Pt}–^{14}\mathrm{N})$ values.

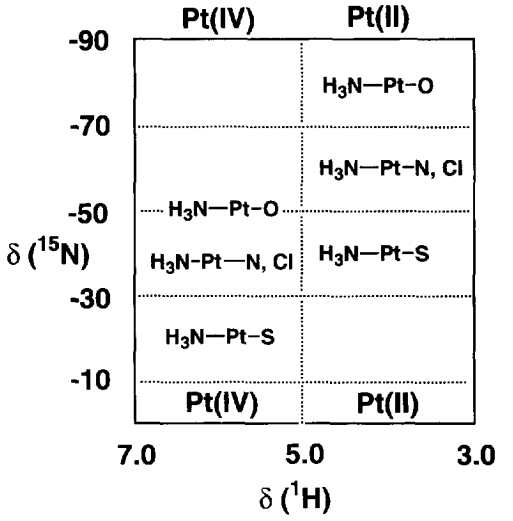

Fig. 6. Variation in ^{1}H and ^{15}N NMR chemical shifts with the *trans* ligand in Pt–NH_3 complexes. A similar picture is obtained for amine complexes, but the shifts are offset in both dimensions, e.g. for ethylenediamine the ^{1}H peaks are shifted to low field by about 2 ppm and ^{15}N shifts to low field by about 40 ppm. Thus not only can Pt(II) be distinguished from Pt(IV) but also Pt–NH_3 from Pt–NH_2 and Pt–NH.

The low receptivity of ^{15}N (3.85×10^{-6} relative to ^{1}H) to some extent limits its usefulness for directly detected ^{15}N NMR studies of Pt ammine and amine complexes. However, the sensitivity of detection can be improved by ^{15}N isotopic enrichment combined with enhancement by polarization transfer from ^{1}H (e.g. ^{15}N–$\{^{1}H\}$ DEPT and INEPT pulse sequences). The maximum enhancement in ^{15}N signal intensity achievable via polarization transfer is only 9.8 ($\gamma H/\gamma N$), but since the repetition time of the pulse sequence is governed by the ^{1}H rather than the longer ^{15}N spin–lattice relaxation time (T_1), there is the additional advantage of allowing more rapid pulsing. For example, ^{15}N–$\{^{1}H\}$ DEPT sequences enable detection of ammine release following reaction of ^{15}N-cisplatin with intracellular components in intact red blood cells at concentrations as low as 1 mM [49].

5.3. *Inverse ^{1}H–$\{^{15}N\}$ NMR*

Over the past few years we have applied inverse (^{1}H-detected) ^{15}N NMR methods to a wide range of studies of platinum anticancer drugs (reviewed in Ref. [50]). The major advantage of the technique is the sensitivity of detection, which is enhanced by a theoretical maximum of 306 ($|\gamma H|/|\gamma N|)^{5/2}$) with respect to directly detected ^{15}N, such that signals can be detected from platinum complexes in aqueous solutions at concentrations of physiological relevance. These methods are widely applicable to any complex which has a ^{15}N atom with a measurable spin–spin coupling to ^{1}H (i.e. ammine, primary and secondary amines, but not tertiary amines). In practice the

best results are obtained with large one-bond couplings (about 73 Hz for $^{15}NH_3$). Although ^1H NMR resonances can be detected from NH protons with ^{14}N present in natural abundance (99.6%), they are often broad because of the quadrupolar relaxation of ^{14}N ($I=1$) (Fig. 7). Also, it is necessary to work in H_2O (as opposed to D_2O), since NH protons in platinum ammine and amine complexes usually exchange with D within minutes. Introduction of ^{15}N by synthetic labelling usually gives rise to a sharp ^1H NMR doublet for a Pt–^{15}NH group in H_2O together with (CSA-broadened) ^{195}Pt satellites (Fig. 8). The resonances move progressively to lower field on changing from Pt–NH_3, to Pt–NH_2 to Pt–NH, and Pt^{IV}–^{15}NH ^1H NMR resonances are to lower field of those of Pt(II). In general, exchange of

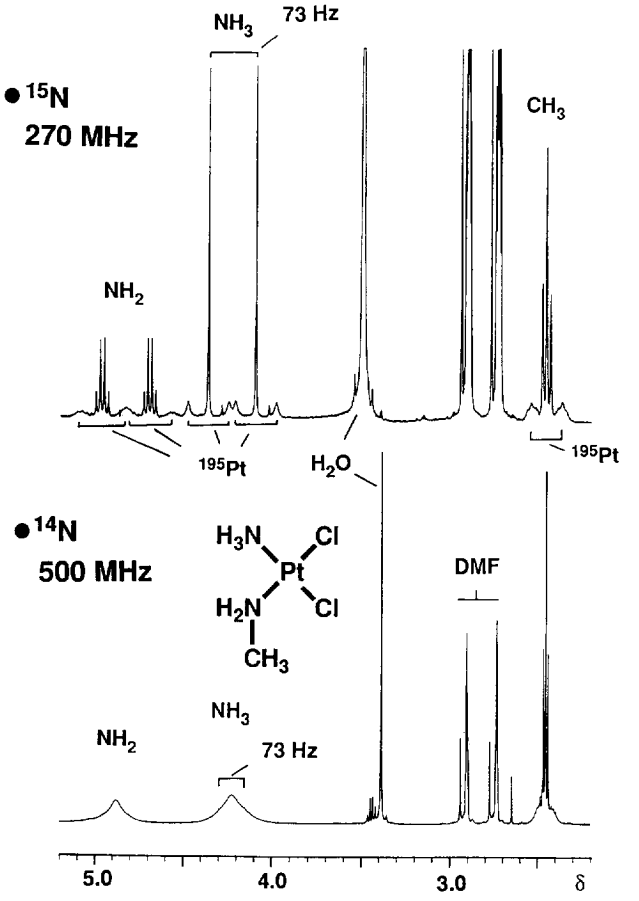

Fig. 7. ^1H NMR spectra of *cis*-[$PtCl_2(NH_3)(NH_2Me)$] in d_6-dimethylformamide: top, with ^{15}N-labelled ligands; bottom, with natural abundance nitrogen in the ligands (0.37% ^{15}N). In this solvent NH exchange is slow and ^1H–^{15}N coupling is clearly evident in the top spectrum. The bottom spectrum shows quadrupolar broadening due to ^{14}N and natural abundance ^{15}N-coupled peaks are just visible. In the top spectrum the ^{195}Pt satellites are broadened by relaxation via chemical shift anisotropy (see text). (Adapted from Ref. [62] (deposited figure).)

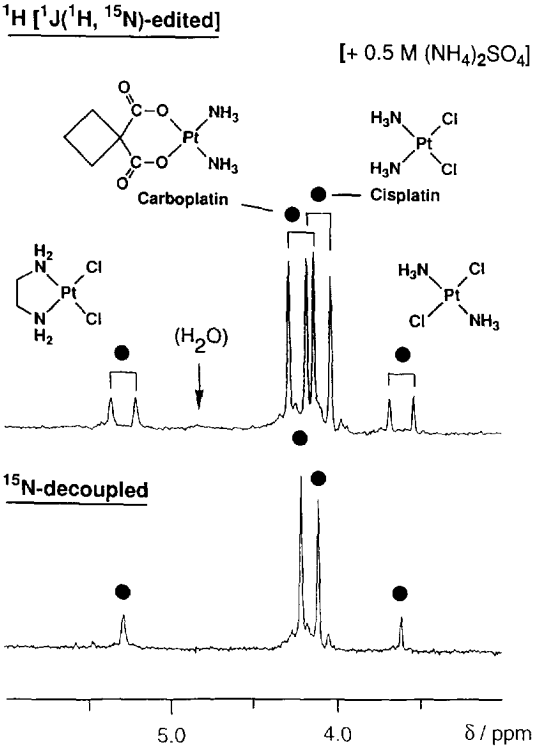

Fig. 8. ^{1}H–{^{15}N} NMR spectra of cisplatin (1), transplatin, carboplatin (2) and [Pt(en)Cl_2] in 95% H_2O–5% D_2O. This method detects only protons bound to ^{15}N and in the top spectrum these appear as doublets due to ^{15}N coupling. The bottom spectrum is ^{15}N decoupled and each different type of NH appears as a singlet (along with broadened ^{195}Pt satellites). In this example ammonium sulphate was added as a relaxation agent to improve water suppression, but a similar suppression could also be achieved using pulsed field gradients.

NH protons with solvent is much faster for Pt(IV) than for Pt(II) complexes, but Pt(IV) anticancer complexes can be studied by ^{1}H–{^{15}N} NMR if the NH exchange is slowed down by lowering the pH or by other means.

The Pt–^{15}NH protons can be detected selectively by the use of heteronuclear single (or multiple) quantum coherence (HSQC and HMQC) pulse sequences (Fig. 9). By acquiring only the first increment in a two-dimensional experiment, a 1D ^{1}H spectrum containing only resonances from Pt–^{15}NH species is obtained; resonances for CH and OH (including water) are eliminated. This is of particular value in studies of body fluids or cell culture media, where it is possible to follow the speciation of the platinum complexes without interference from the thousands of other overlapping ^{1}H resonances, which are completely filtered out. If ^{15}N decoupling is employed during acquisition (e.g. the GARP method), then each distinct type of Pt–NH resonance appears as a singlet, sometimes together with the broadened ^{195}Pt satellites (Fig. 8). In practice the water resonance is so intense that it is usually necessary to

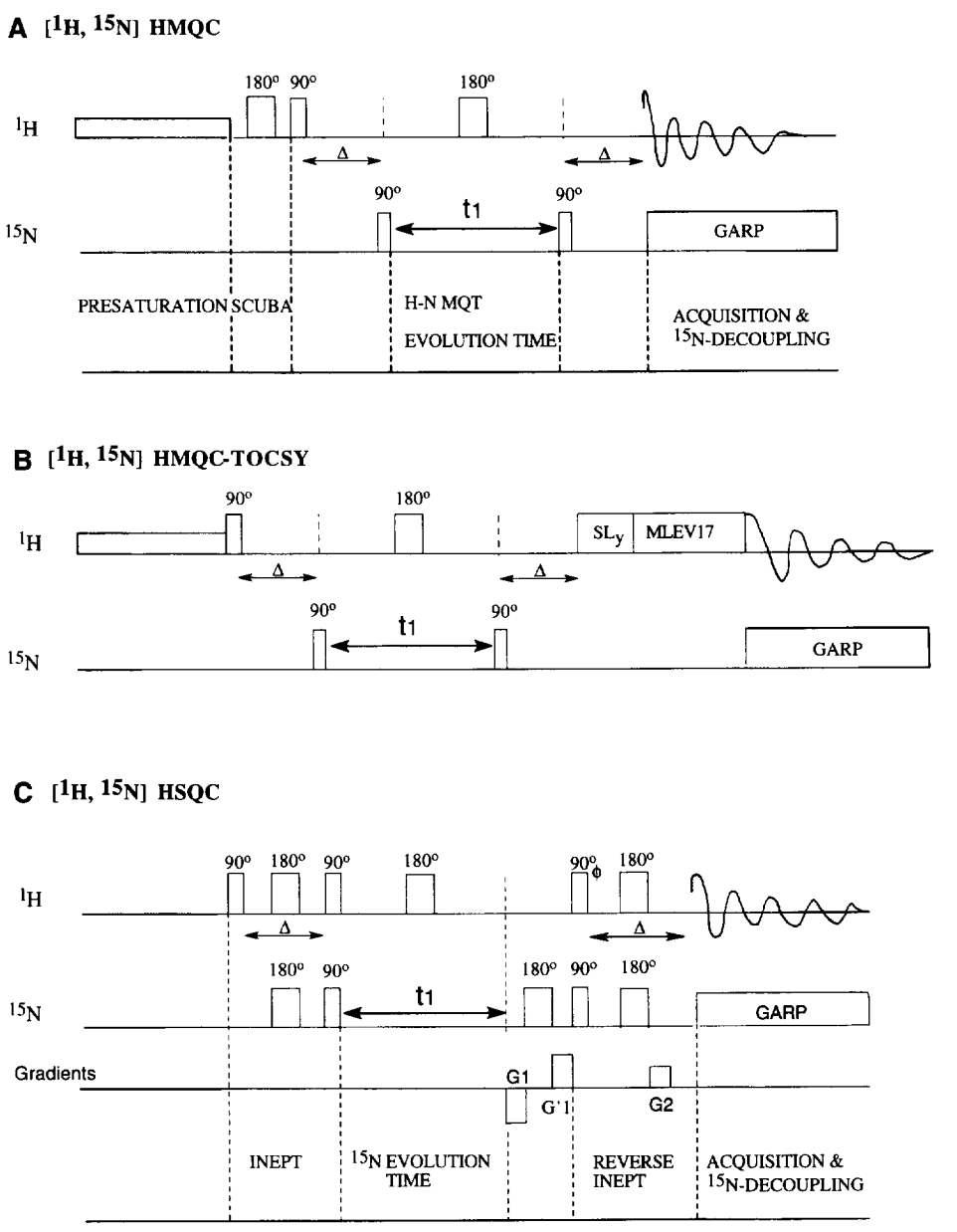

Fig. 9. Examples of pulse sequences used to record [^{1}H, ^{15}N] spectra of Pt–NH systems in 95% H_2O–5% D_2O. In all cases the delay $\Delta = \frac{1}{2}J(N,H)$ and one-dimensional ^{15}N-edited ^{1}H spectra are obtained by setting the evolution period (t_1) to zero. Spectra may be recorded with or without decoupling of ^{15}N spins (GARP) during the acquisition period. (A) [^{1}H, ^{15}N] HMQC sequence [90] in which the water signal is suppressed by presaturation. Other modifications are usually needed to improve the suppression and to detect peaks close to the ^1H_2O resonance, e.g. the addition of purge pulses as described by Otting and Wüthrich [91]. Incorporation of a SCUBA sequence [92] in the preparation period is useful for

use additional solvent suppression techniques (e.g. presaturation; Fig. 9A). The addition of an H_2O T_2 relaxation agent (e.g. 0.5 M $(NH_4)_2SO_4$) [51] can also be useful if the NH peaks of interest lie very close to the ^1H_2O peak. However, the use of pulse sequences in which coherence selection is achieved by the use of pulsed field gradients allows greatly improved water suppression. For example, by use of the HSQC sequence of Stonehouse *et al.* [52] (Fig. 9C) we have been able to detect NH peaks within a few hertz of the water resonance at concentrations as low as about 10 μM without the need for additional solvent suppression techniques. Acquisition of ^{15}N-coupled spectra can aid in the detection of Pt–NH species if the ^{15}N-decoupled NH peak is obscured by the small residual ^1H_2O signal.

The combined detection of ^1H and ^{15}N in a 2D inverse NMR experiment is especially powerful, since the ^{15}N NMR chemical shift and the one-bond coupling constant $^1J(^1H–^{15}N)$ are diagnostic of the trans ligand (vide supra). In a 2D [^1H, ^{15}N] spectrum the ^{195}Pt satellites (when not broadened beyond detection by the effects of CSA relaxation) appear on a diagonal corresponding to the $^2J(^{195}Pt–^1H)$ coupling constant in the F_2 (^1H) dimension and to the $^1J(^{195}Pt–^{15}N)$ coupling in the F_1 (^{15}N) dimension (Fig. 10). Pt(II) and Pt(IV) ammine and amine complexes can be distinguished by the combination of ^1H and ^{15}N shifts (Fig. 6).

By appending a proton isotropic mixing sequence to the basic HMQC (or HSQC) sequence (Fig. 9B), magnetization is relayed from the NH protons to the other protons in the spin system, providing a further tool for the assignment of NH protons in differently coordinated environments. For example, Fig. 11 shows the 2D HMQC–TOCSY spectrum of the product of the reaction of $[Pt(^{15}N\text{-en})(H_2O)_2]^{2+}$ with ^{15}N-labelled L-methionine (^{15}N-L-MetH). The NH_2 protons of both ethylenediamine (en) and methionine have chemical shifts between 5 and 6 ppm and the highly overlapping multiplets in 1D spectra (Fig. 11B) cannot easily be analysed. The 2D HMQC–TOCSY spectrum contains cross-peaks showing the connectivity between the methionine NH proton and the $C_\alpha H$, $C_\beta H$ and $C_\gamma H$ protons of the side-chain and between the ethylenediamine NH and CH_2 bridge protons. This allows unambiguous assignment of resonances for coordinated methionine–NH and en–NH and identification of $[Pt(^{15}N\text{-en})(\text{L-Met H-}S,N)]^{2+}$ as the major product of the reaction.

[^1H, ^{15}N] NMR spectroscopy is of particular value in following the pathways of reactions of platinum ammine and amine complexes. It has the advantage that all Pt–NH species are detected simultaneously without the need for trapping out reac-

---

restoration of magnetization which would otherwise be affected by the suppression. (B) [^1H, ^{15}N] HMQC–TOCSY sequence [93] in which a proton isotropic mixing sequence (MLEV-17) is appended to the basic HMQC sequence to relay magnetization from the NH protons to other protons in the spin system (see text). (C) [^1H, ^{15}N] HSQC sequence in which coherence selection is achieved by the use of pulsed field gradients. The gradients G1, G'1 and G2 are in the ratio $-5:5:1$ (controlled with either amplitude or time) in accordance with the requirement $(|G1|+|G'1|)/G2=\gamma H/\gamma N$ (9.88). Gradient sequences greatly improve solvent suppression so that NH peaks can be detected very close to the ^1H_2O peak without the need for additional water suppression techniques. If the phase (ϕ) of the final proton pulse is set to x, the water magnetization is returned to the z axis (its equilibrium position) prior to the relaxation delay. This minimizes the loss in signal intensities of NH protons which are in exchange with water [52]. Note that the phases of all other pulses have been omitted for clarity.

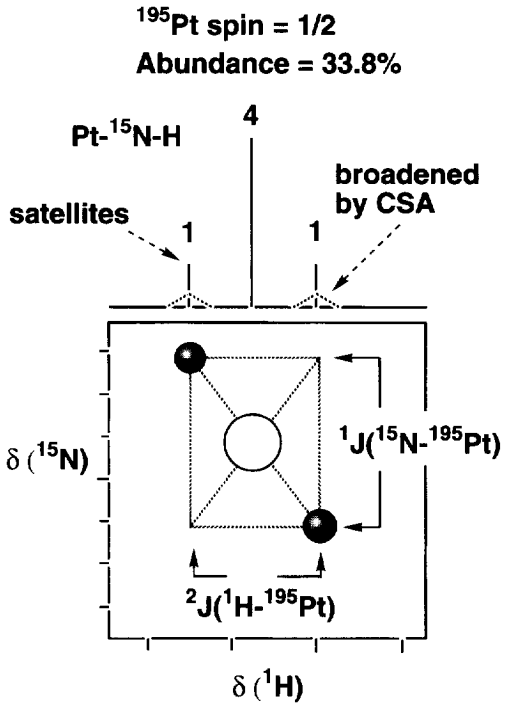

Fig. 10. General appearance of a 2D [^{1}H, ^{15}N] HMQC or HSQC spectrum. The ^{195}Pt satellites are usually more intense for symmetrical Pt species, i.e. satellites for Pt(IV) complexes are more readily observed than those for Pt(II) complexes.

tion intermediates or chromatographic separation of products. It takes only a few minutes to acquire a 1D ^{15}N-edited ^{1}H spectrum at millimolar concentrations and pathways can be followed by observing time-dependent changes in the intensity of the Pt–NH ^{1}H resonances and by recording 2D [^{1}H, ^{15}N] spectra at selected time intervals to allow assignment of Pt–N–H species *via* their ^{15}N chemical shifts. For example, we have investigated the pathways of reactions of ^{15}N-cisplatin with the decamer oligonucleotide d(ACATGGTACA) and with the duplex containing the complementary strand [53]. This has allowed us to determine directly for the first time the lifetime of the aqua-chloro intermediate (8 min) and to observe the formation of monofunctional and bifunctional adducts in a single experiment. One of the monofunctional adducts is present during the course of the reaction to a greater extent than the other, in line with the findings of Gonnet et al. [54] and there is a preferential rate of ring closure (the platinated 3′-G ring closing faster to 5′-G). It should be possible to use these methods to study the platination of much longer strands of DNA.

By observation of ^{1}H and ^{15}N NMR chemical shifts as a function of pH, we determined the pK_a values of both the cisplatin hydrolysis products *cis*-$[PtCl(H_2O)(NH_3)_2]^+$ (6.41) and *cis*-$[Pt(H_2O)_2(NH_3)_2]^{2+}$ (5.37 and 7.21) [55].

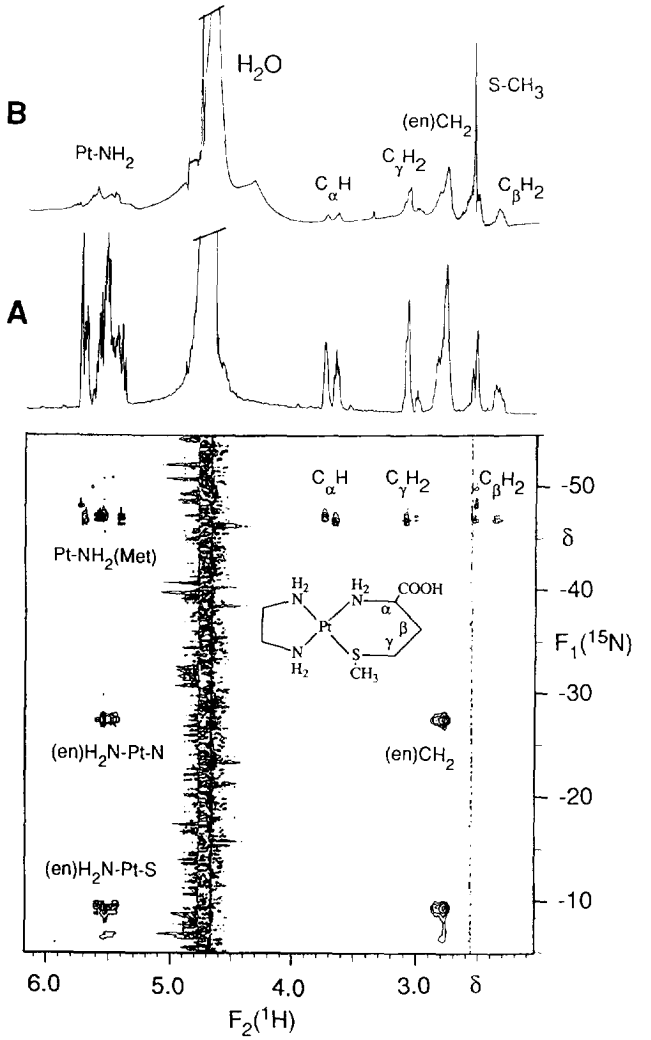

Fig. 11. 2D [^{1}H, ^{15}N] HMQC spectrum, with TOCSY transfer (mixing time 67 ms), of [Pt(^{15}N-en)(L-Met H-*S*,*N*)]$^{2+}$ prepared by mixing [Pt(^{15}N-en)(H_2O)$_2$]$^{2+}$ and ^{15}N-L-methionine in a 1:1 molar ratio for 72 h at 37 °C (pH 2.1). (A) is the projection of the F_2 (^{1}H) dimension and (B) is the ^{1}H spectrum of the solution obtained by normal single-pulse acquisition (with presaturation of the ^1H_2O resonance). Slow inversion of the chiral coordinated sulphur (on the NMR time scale) gives rise to two sets of peaks (resolved for Met NH_2). The SCH_3 peak does not appear in the 2D spectrum because it is a singlet and is not scalar coupled.

These titrations can be carried out at low concentration (millimolar) and any hydroxo-bridged species which form during the course of the reaction can be readily detected. In principle the pK_a values of aqua ligands on any Pt(II) ammine or (primary or secondary) amine complex can be determined by the same method. Such

information is valuable in understanding structure–activity relationships because of the reactivity of bound aqua ligands but inertness of hydroxo ligands.

[^{1}H, ^{15}N] NMR methods offer enormous potential for characterizing the metabolites of platinum drugs in intact body fluids, since it is possible to detect metabolites in animal urine after the administration of ^{15}N-labelled Pt complexes. ^{15}N editing removes background interference from other substances in urine, so that detection limits are very low (10 μM). For example, the spectra of urine of mice treated with ^{15}N-carboplatin have ^{1}H and ^{15}N peaks characteristic of a complex with NH_3 trans to O and S, which may be related to the ring-opened complex [$Pt(NH_3)_2$(CBDCA-*O*)(L-Met-*S*)], which has similar shifts (Fig. 12) [56]. Ring-opened S-bound L-methionine adducts of carboplatin are surprisingly stable despite the ease of L-Met S,N ring closure with displacement of CBDCA. The half-life of [$Pt(NH_3)_2$(CBDCA-*O*)(L-Met-*S*)], for example, is about 1 day at 37°C [57]. In preliminary experiments on the urine from animals treated with ^{15}N-cisplatin [58], we have detected about 20 different types of Pt–NH_3 species, including at least four with sulphur as the trans ligand (thioethers and thiols).

One of the few characterized metabolites of cisplatin is the complex [Pt(L-Met)$_2$] which was isolated from the urine of patients over 10 years ago [59]. Then it was described as having the trans geometry. The complex is readily produced during chemical reactions of cisplatin with L-Met and by the use of ^{15}N-labelling we have characterized it in detail by ^{1}H and ^{15}N NMR spectroscopy. In solution, [Pt(L-

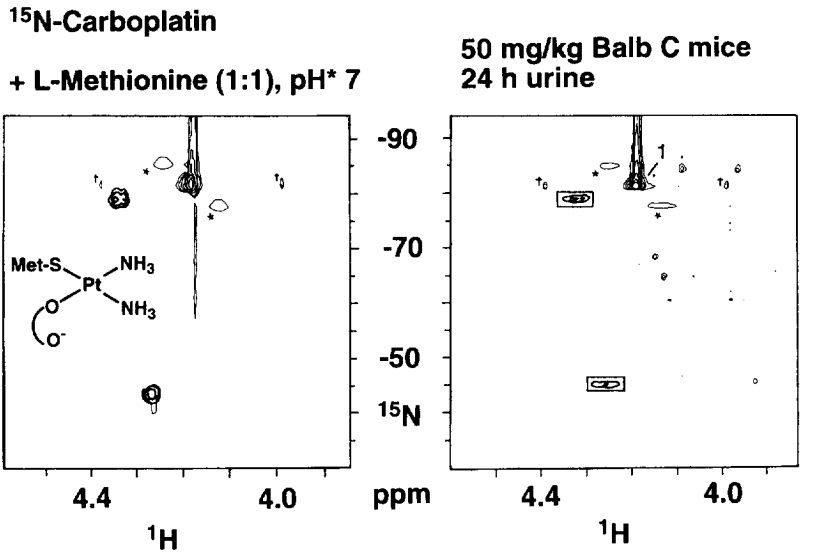

Fig. 12. [^{1}H, ^{15}N] HMQC NMR spectra of a solution containing the anticancer drug carboplatin (**2**; labelled 1 in the figure) (^{15}N labelled) and L-methionine in a 1:1 molar ratio 3.5 h after mixing (left) and of urine collected from mice treated with ^{15}N-carboplatin (right). The marked similarity of the shifts for the boxed peaks in the spectrum of urine to those for the model complex shown on the left strongly suggests that a complex similar to the ring-opened complex shown is excreted in urine. (Adapted from Ref. [56].)

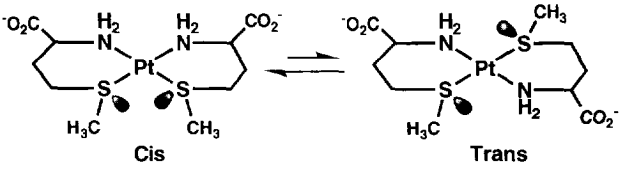

Scheme 2

$Met)_2$] exists as a mixture of cis and trans isomers (Fig. 5, Scheme 2), the former predominating by about 87:13, and each of these exists as a further three diastereomers owing to the presence of two chiral coordinated S atoms [60,61]. The *cis* and *trans* isomers can be separated by high performance liquid chromatography (HPLC), but the inversion of S is too rapid to allow separation of the diastereomers. The combination of [^{1}H, ^{15}N] NMR with chromatography should be a powerful one for identification of novel Pt metabolites.

A further important aspect of inverse ^{1}H–{^{15}N} NMR techniques is that they allow *direct* study of the N–H bonds in platinum anticancer complexes in aqueous solutions. These N–H bonds are thought to play a crucial role in the mechanism of action of platinum drugs and hydrogen bonds between the N–H protons and e.g. C6O and 5′-phosphates of DNA nucleobases may strongly influence the kinetics of reactions and contribute to the preference of Pt for particular bases and cross-links. Although such H-bonding interactions have been clearly demonstrated in the solid state, they had previously been detected in solution only indirectly. We used ^{1}H–{^{15}N} NMR methods to study H-bonding interactions of N–H protons in $^{15}NH_3$- and ^{15}N-ethylenediamine Pt(II) complexes with G and A purine bases with various sites of phosphorylation (3′ or 5′) in aqueous solutions [62]. Significant low field shifts of N–H protons were found to be diagnostic of stereospecific H-bonding between the N–H protons and *cis* nucleotide 5′-phosphate groups in head-to-tail mononucleotide complexes [$Pt(en)X_2$] (e.g. X is 5′-GMP, 5′-dGMP, 5′-AMP). Similarly, strongly deshielded NH ^{1}H resonances provide strong evidence for the presence of PtNH$\cdots$ 5′-phosphate H bonding when there is a terminal 5′-phosphate present in an oligonucleotide, as in pGpG adducts but not for GpG or TpGpG adducts [63].

A large low-field shift was observed for one of the Pt–NH_3 resonances of the platinated GG adduct of the single-stranded decamer oligonucleotide d(ACATGGTACA). A similar shift was observed for the GG platinated duplex just after it melted, suggesting that a GG platinated single-strand lesion still possesses secondary structure. The ^{1}H and ^{15}N shifts of Pt–NH_3 resonances provide a new monitor for cisplatin-induced helix melting [53].

6. Interaction of metallodrugs with blood plasma proteins

The major metal transport proteins in the blood are serum albumin (66 kDa, concentration about 0.63 mM) and transferrin (80 kDa, concentration about 35 μM).

^{1}H NMR studies on these high molecular mass proteins are complicated by the overlap of the very large number of resonances. The sharpest peaks in the spectra are from the more mobile regions, including loops and the N terminus. Other resolvable peaks include those in the high-field-shifted methyl region (0 to −2 ppm) from groups lying over the faces of aromatic rings of side-chains such as Trp, Phe and Tyr. In the case of transferrin one such region consists of a hydrophobic patch in helix 5 close to the metal site.

A useful approach in simplifying these complicated spectra is to use resolution enhancement techniques, although this has to be done with care, because broad peaks are removed from the spectra. For these proteins a combination of sine bell and exponential functions applied to the free induction decay is often helpful. Moreover, ^{1}H NMR peaks for albumin are assignable in spectra of intact blood plasma and this allows competitive metal binding to be investigated directly in blood plasma. Isotopic labelling with ^{13}C or ^{15}N can be used to simplify the spectra and aid assignments and some direct studies of metal nuclei are also possible.

6.1. Albumin

Albumin is a single-chain protein which is largely α-helical. It is composed of three structurally similar domains of about 22 kDa and each of these has six disulphide bridges, except for domain I, the N-terminal domain, which is missing one cysteine residue and consequently has a free thiol group at Cys34. Metal ions transported by albumin include the essential metals Ca(II), Zn(II), V(IV), Ni(II) and Cu(II) and metals which enter the body in drugs or as xenobiotics, including Au(I), Hg(II) and Cd(II).

6.1.1. N-Terminal Cu(II) and Ni(II) site

^{1}H NMR resonances for the N-terminal residues of albumin Asp1-Ala2-His3-Lys4- can be assigned in spectra of both isolated albumin and human blood plasma. There is a strong square-planar binding site for both Ni(II) and Cu(II) consisting of the amino terminus, two deprotonated peptide nitrogen atoms and the imidazole δN of His3 [64] (Fig. 13A). Since square-planar Ni(II) is diamagnetic, ^{1}H NMR resonances can be observed for Ni(II)–albumin [65]. The most interesting feature of the ^{1}H NMR coordination shifts of these residues is the pattern for Lys4 even though this is not a metal ligand. This can be explained on the basis of ring current calculations by assuming that the side-chain of Lys4 lies over the coordinated imidazole ring of His3, much as in the X-ray crystal structure of [Cu^{II}(Gly-L-His-L-Lys)] [66]. This interaction may be important to the biological properties of Ni–albumin, which is known to be the antigenic determinant in cases of Ni allergy, a condition which affects some 5–10% of the general population. ^{1}H NMR studies of human blood plasma show that Ni(II) complexation induces a similar structural

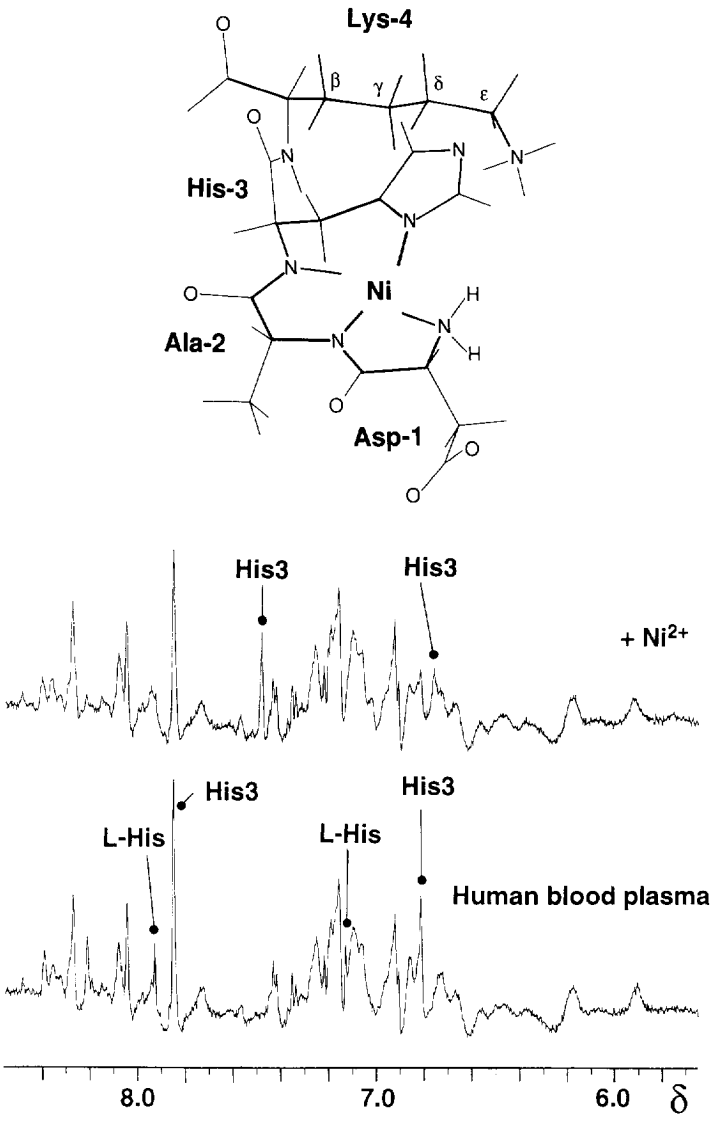

Fig. 13. (A) The square-planar N-terminal site for Ni(II) and Cu(II) in human serum albumin showing metal coordination to the amino terminus, deprotonated peptide nitrogen atoms and imidazole nitrogen. NMR data suggest that the side-chain of Lys4 lies over the imidazole ring of coordinated His3. (Adapted from Ref. [67].) (B) Detection of Ni(II) binding in the above site in intact human blood plasma by (resolution-enhanced) ^{1}H NMR spectroscopy. Note that some binding of Ni(II) to the free amino acid L-histidine also occurs. Whereas the Ni–albumin complex is diamagnetic and therefore gives sharp NMR peaks, the Ni^{II}–L-His complex is paramagnetic and its peaks are broadened and shifted outside this spectral range.

change in albumin in intact blood plasma to that observed for isolated albumin [67]. In plasma the amino acid L-histidine competes with albumin for Ni(II) binding (Fig. 13B).

6.1.2. Gold binding at Cys34

Albumin is the major transport protein for gold in patients treated with antiarthritic drugs and the strong binding site is located at Cys34 [24]. Unexpectedly, gold(I) binding to Cys34 of albumin causes a change in the environment of His3, such that new δCH and εCH ^{1}H imidazole resonances appear in the spectrum in slow exchange with resonances for His3 of the apoprotein [68]. This structural change can be associated with a movement of Cys34. In the X-ray crystal structure [69], Cys34 is in a cleft, apparently stabilized in the ionized Cys-S$^-$ form ($pK_a \approx 5$ [70]), probably via H bonding to His39. When gold binds, it moves to a more solvent-exposed position and evidently this structural change is communicated along the intervening helices to His3, part of the strong N-terminal square-planar Ni(II) and Cu(II) site. Such a structural switch can also be induced by blocking Cys34 as a disulphide, e.g. with cystine [71]. This and Au(I) binding can be reversed by adding thiols to blocked albumins. In blood, these events may be important for the regulation of the redox state of plasma and for the recognition of albumin by receptors and eventually its removal from circulation.

^{1}H NMR spectroscopy can also be used to detect structural switches of albumin induced by the gold drugs auranofin and aurothiomalate directly in human blood plasma [71]. At low pH (6) the switch is not quantitative, since the added thiols (thiomalate and thioglucose) are competitive with Cys34 for Au(I). This can be accounted for by the protonation of Cys34.

6.2. Transferrin

The major role of transferrin in the blood is to transport iron as Fe(III) to many types of cell in the body. Transferrin is a single-chain glycoprotein composed of two structurally similar lobes (the N-lobe and C-lobe, about 40 kDa each). Human transferrin has two biantennary glycan chains in the C-lobe (attached to Asn413 and Asn611). Each lobe is composed of two domains with alternating α-helical and β-sheet structures and Fe(III) binds in a deep cleft between the two domains [72]. An intriguing feature of the metal binding is that Fe(III) binds only when accompanied by a synergistic anion. This is probably carbonate in blood but in vitro can be other anions such as oxalate. The iron-binding ligands in both lobes are oxygen atoms from an aspartate, two tyrosinates and a bidentate carbonate (synergistic anion) and εN from the imidazole ring of His (Fig. 14). When Fe(III) binds, the interdomain cleft closes tightly and transferrin has therefore been classified as a "Venus fly-trap" protein [72].

The recognition of transferrin by cells is a highly specific process. Only diferric transferrin (i.e. Fe(III) in both the N-lobe and C-lobe sites) and not the apoprotein is recognized by receptor proteins on the surfaces of cells and is taken up. Inside

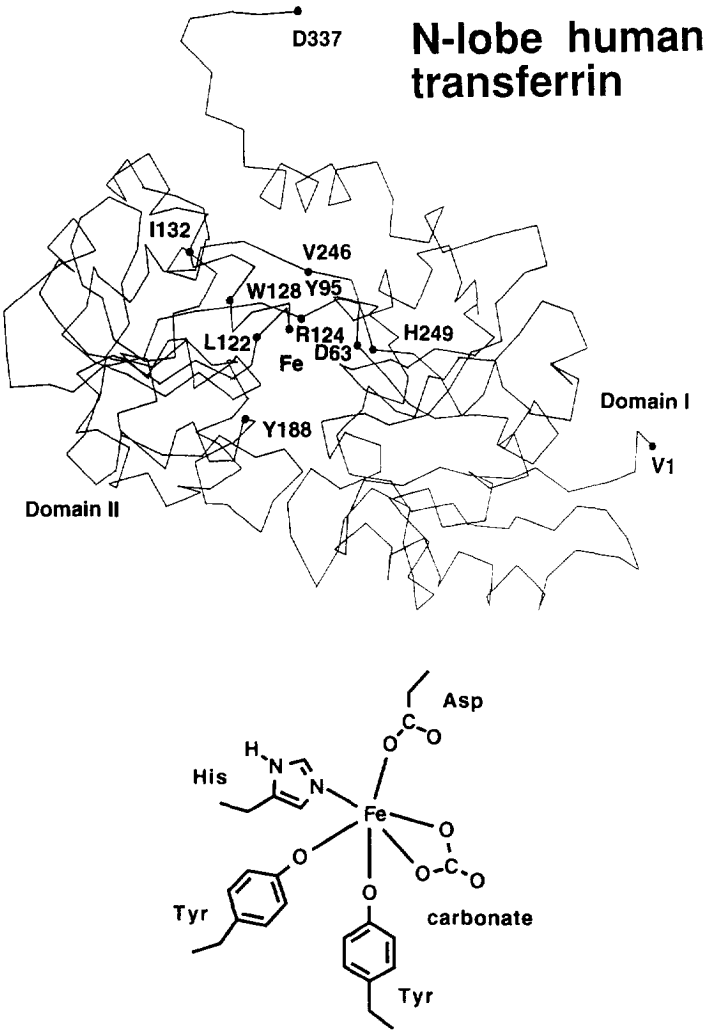

Fig. 14. (A) Model of the N-lobe of human serum transferrin showing the interdomain metal-binding site and location of helix 5 containing amino acid residues Leu122 and Ile132 which give rise to high-field-shifted ^{1}H NMR resonances. (Adapted from Ref. [88].) (B) The metal-binding site of transferrin. A similar site exists in both the N- and C-lobes and is composed of the synergistic anion (carbonate) together with ligands from domain I (Asp, His), domain II (Tyr) and the interdomain hinge (Tyr).

cells it is placed in membrane-bound vesicles (endosomes) where the pH is lowered to about 5.5 and Fe(III) is released. The apoprotein remains bound to its receptor protein at pH 5.5 and is transported back to the surface of the cell. At an extracellular pH of 7.4 it dissociates from the receptor, is released into the blood and reutilized.

Because the interdomain metal-binding cleft of transferrin is hinged, a wide variety of metal ions of differing ionic size can be accommodated in the iron site. These include:

Metal ion	Radius (Å)	Metal ion	Radius (Å)
Al^{3+}	0.54	Sc^{3+}	0.75
Ga^{3+}	0.62	In^{3+}	0.80
Fe^{3+}	0.65	Cd^{2+}	0.95
Zn^{2+}	0.74		

The stabilities of complexes of these metals with transferrin vary over a wide range (Table 2), the most stable being the Fe^{3+} complexes followed by Ga^{3+} and In^{3+} [73–77]. The affinities of the two lobes for metal ions are similar, usually one being 10–20 times higher than that of the other. In the blood, transferrin is normally only about 30% saturated with iron and so other metal ions which enter the blood can

Table 2
Conditional stability constants for metal binding to human serum transferrin (pH 7.4, 5 mM bicarbonate); data from Refs. [73–77]

Metal ion	$\log K_1$	$\log K_2$
Cd(II)	5.95	4.86
Zn(II)	7.8	6.4
Al(III)	13.5	12.5
In(III)	18.52	16.64
Ga(III)	20.9	19.3
Fe(III)	22.8	21.5

Table 3
Chemical shift differences (ppm) between N-lobe and C-lobe for various metal nuclei bound to serum transferrin or ovotransferrin; data from Refs. [78–81]

Nucleus	Transferrin	Synergistic anion	δ(N-lobe) − δ(C-lobe)
^{27}Al	Ovo	Carbonate	2.2
		Oxalate	2.0
	Serum	Carbonate	0
^{45}Sc	Ovo	Carbonate	8
	Serum	Carbonate	0
^{51}V	Serum	Carbonate	−2.0
^{113}Cd	Serum	Carbonate	5.5
^{205}Tl	Serum	Carbonate	20

readily bind. There is interest in understanding both the thermodynamic and kinetic selectivities of the N- and C-lobes towards metals and synergistic anions. Since there are potentially large structural changes involved in the metal uptake and release, kinetic control may play an important role.

Multinuclear NMR using diamagnetic metal ions can provide a method for determining which lobe has the higher affinity for metals [78–82]. Thus for ^{205}Tl ($I=\frac{1}{2}$) there is a 20 ppm shift difference between N- and C-lobe binding, although for the quadrupolar nucleus ^{27}Al there is no shift difference for serum transferrin but a small one (2 ppm) for ovotransferrin; see Table 3. Resonances of half-integer quadrupolar nuclei bound to transferrin are much sharper when recorded at very high magnetic field. In the limit of slow isotropic molecular motion (as is the case for these nuclei bound to transferrin or its N-lobe) the linewidth of the central $m=\frac{1}{2}\rightarrow-\frac{1}{2}$ transition decreases with increasing magnetic field:

$$\Delta\nu_{\frac{1}{2}}=k\,\chi^2\sqrt{\nu_0^{-2}\tau_c^{-1}}$$

where χ is the quadrupolar coupling constant, τ_c is the correlation time of fluctuations in the electric gradient at the nucleus and ν_0 is the resonance frequency (which is proportional to the magnetic field). This central transition dominates the spectrum whereas the other components are broadened at high field. For example, the linewidth of the ^{71}Ga–N-lobe of ovotransferrin decreases from 1900 Hz at 11.7 T to 860 Hz at 17.6 T. It should be noted that in these quadrupolar systems the chemical shifts are field dependent (second-order dynamic frequency shift) according to

$$\Delta\delta_d=-k\,\chi^2\sqrt{\nu_0^{-2}}$$

For ^{71}Ga ($I=3/2$), $k=2.0\times10^{-2}$ and the chemical shift is -19 ppm at 11.7 T but -57 ppm at 17.6 T [9].

Transferrin is believed to be responsible for the delivery of radioactive γ-emitter ^{67}Ga to tumour tissues, allowing diagnostic radio-imaging studies to be carried out. It is notable that $[Ga(NO_3)_3]$ has anticancer activity in its own right [83]. Tumour cells have a large number of transferrin receptors on their surfaces and it may be possible to deliver a range of metal ions to tumour cells in this way. One example is ruthenium.

Kratz et al. [84] have reported that the antitumour complex $[RuInd_2Cl_4]^-$ (Ind means indazole) forms well-defined complexes with human apotransferrin within a few minutes of mixing in solution, whereas the related complex $[RuCl_4Im_2]^-$ (**3**) (Im means imidazole) reacts much more slowly. They have shown by X-ray crystallography that Ru binds to the imidazole ring of the His residue in the iron-binding site, probably with loss of one of the chloride ligands. The indazole complex retains its activity against colon cancer cells when bound to apotransferrin.

^1H NMR studies of transferrin are complicated by the broadness of the resonances (high M_r, slow tumbling) and the severe overlap problem (large number of protons). Nevertheless, with the aid of resolution enhancement, resonances for most of the His residues can be resolved and pH titration curves established [85]. In the high field

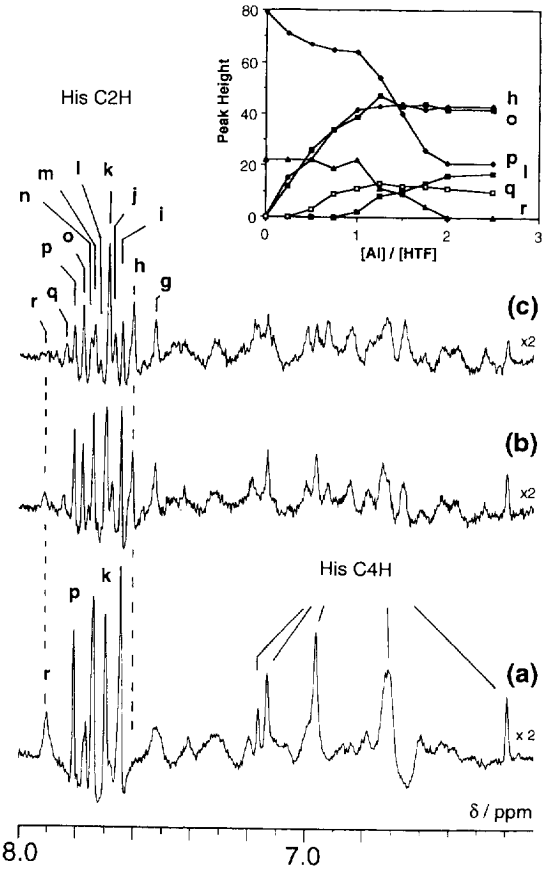
His C2H
Peak Height
[Al] / [HTF]
h
o
p
l
q
r
m
l
k
n
j
i
p
o
h
g
r
q
(c)
x2
(b)
x2
His C4H
p
k
r
(a)
x 2
δ / ppm
8.0
7.0

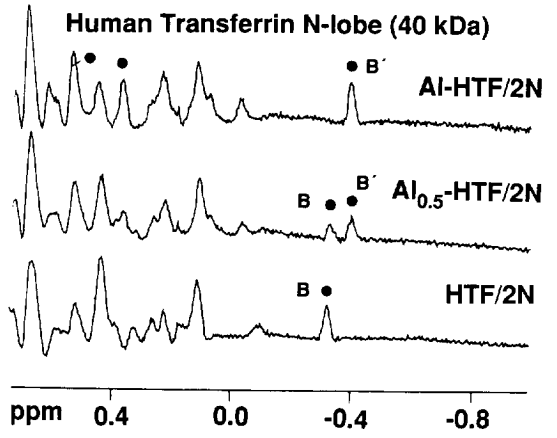
Human Transferrin N-lobe (40 kDa)
B´
Al-HTF/2N
B
B´
Al0.5-HTF/2N
B
HTF/2N
ppm
0.4
0.0
-0.4
-0.8

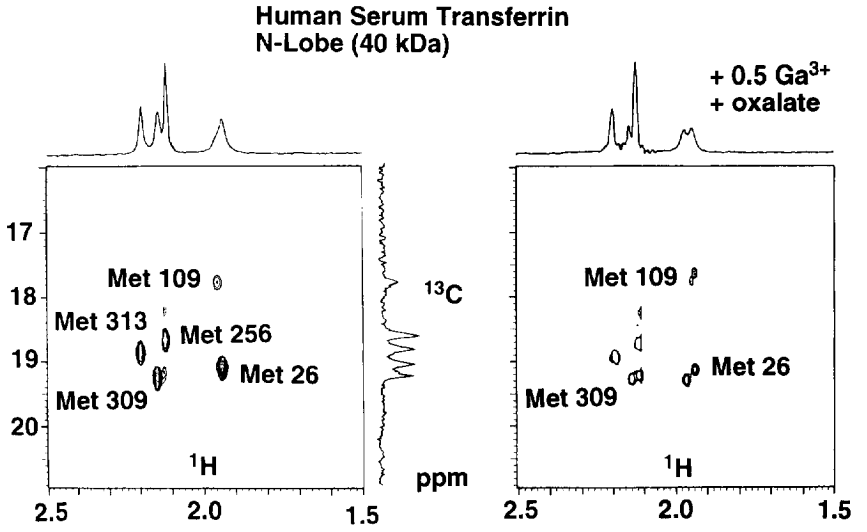

Fig. 16. 2D [^{1}H, ^{13}C] HMQC NMR spectra of the N-lobe of serum transferrin (40 kDa) which has all five SCH_3 groups of its methionine residues labelled with ^{13}C. It can be seen that Met26, Met109 and Met309 are all perturbed by Ga^{3+} binding even though they are more than 15 Å from the metal site. (Adapted from Ref. [89].)

region of the spectrum (0 to −3 ppm), peaks for ring-current-shifted methyl groups can be resolved. The sharpest peaks in the spectrum (near 2 ppm) belong to the N-acetyls of the glycan chains in the C-lobe. Al^{3+} and Ga^{3+} both bind tightly to apotransferrin and resonances for free and bound transferrin are in slow exchange on the ^{1}H NMR time scale when these ions are titrated into solutions of the protein. By comparing the pattern of shift changes for transferrin itself with those seen for the isolated recombinant N-lobe, it is possible to determine the order of metal loading of the lobes (N or C) with e.g. Al^{3+} or Ga^{3+} (Fig. 15) [86,87]. With carbonate as synergistic anion, Al^{3+} appears to bind more strongly to the N-lobe, whereas with oxalate as anion, Ga^{3+} is taken up preferentially by the C-lobe. Certain resonances in the spectrum of apotransferrin are sensitive to the binding of synergistic anions and this allows anion-binding constants to be determined, e.g. log $K=4$ for oxalate binding to the apo-N-lobe. Metal ion binding to apotransferrin or the recombinant apo-N-lobe can be conveniently monitored via shifts of high-field-shifted methyl resonances assignable to Ile132 and Leu122 (Fig. 15B) which are in close contact with either side of the indole ring of Trp128 [88]. Together these

Fig. 15. (Top) The aromatic region of resolution-enhanced 500 MHz ^{1}H NMR spectra of human transferrin (80 kDa) showing the sequential loading of the N-lobe and then the C-lobe with Al^{3+} at pH* 8.8 with carbonate as synergistic anion: (a) apo-HTF, (b) +1.25 mol equiv. Al^{3+} and (c) +2.5 mol equiv. Al^{3+}. (Adapted from Ref. [86].) (Bottom) Resolution-enhanced 500 MHz ^{1}H NMR spectra of the N-lobe of human serum transferrin (40 kDa) and on addition of 0.5 and 1.0 mol equiv. Al^{3+} showing the slow exchange of apo and Al-bound protein. The peak labelled B is assigned to Leu122, a residue in helix 5 which contacts the synergistic anion-binding site. (Adapted from Ref. [88].)

residues form a hydrophobic patch in helix 5 of the N-lobe which is in close contact with the metal-binding site (Fig. 14).

Isotopic labelling is a promising method for providing assignments of resonances for specific amino acid residues of transferrin. For example, it is possible to use [^{1}H, ^{13}C] HMQC–NOESY experiments to assign the S–$^{13}CH_3$ resonances of all five Met residues of the N-lobe (Fig. 16). Three of these (Met26, Met109 and Met309) are sensitive to Ga^{3+} binding even though they are distant from the metal site [89]. We are extending these labelling studies to the intact 80 kDa protein.

Acknowledgements

We thank the Australian NH&MRC (R. Douglas Wright Award to S.J.B.-P.), the MRC, BBSRC, EPSRC, Royal Society, Association for International Cancer Research, Wellcome Trust, British Council, Delta Biotechnology, Glaxo and EC (HCM and COST) for their support for various aspects of our work. We are grateful to the MRC and ULIRS for the provision of NMR facilities.

References

[1] P.J. Sadler, in M. Nicolini and L. Sindellari (eds.), Lectures in Bioinorganic Chemistry, Cortina Int./Raven, Verona/New York, 1991, p. 1.
[2] M.J. Abrams and B.A. Murrer, Science, 261 (1994) 725.
[3] P.J. Sadler, Adv. Inorg. Chem., 36 (1991) 1.
[4] B.K. Keppler (ed.), Metal Complexes in Cancer Chemotherapy, VCH, Weinheim 1993.
[5] C. Luschinsky Drennan, S. Huang, J.T. Drummond, R.G. Matthews and M.L. Ludwig, Science, 266 (1994) 1669.
[6] F.P. Dwyer, E.C. Gyarfas, R.D. Wright and A. Shulman, Nature (Lond.), 197 (1957) 425.
[7] P.G. Farnworth, A. Shulman and A.T. Casy, Chem.-Biol. Interact., 18 (1977) 289.
[8] F. Kayser, M. Biesemans, M. Gielen and R. Willem, J. Magn. Reson. A., 102 (1993) 249.
[9] M.W. Germann, J.M. Aramini and H.J. Vogel, J. Am. Chem. Soc., 116 (1994) 6971.
[10] S.J. Berners-Price, R.K. Johnson, C.K. Mirabelli, L.F. Faucette, F.L. McCabe and P.J. Sadler, Inorg. Chem., 26 (1987) 3383.
[11] O.M. Ni Dhubhghaill and P.J. Sadler, Struct. Bond., 78 (1991) 129.
[12] E. Asato, W.L. Driessen, R.A.G. de Graaff, F.B. Hulsbergen and J. Reedijk, Inorg. Chem., 30 (1991) 4210.
[13] E. Asato, K. Katsura, M. Mikuriya, T. Fujii and J. Reedijk, Inorg. Chem., 32 (1993) 5322.
[14] P.J. Sadler and H. Sun, J. Chem. Soc. Dalton Trans., (1995) 1395.
[15] P.J. Sadler H. Sun and H. Li, Chem. Eur. J. (Angew. Chemie), 1996, in press.
[16] R.B. Lauffer, Chem. Rev., 87 (1987) 901.
[17] O.M. Ni Dhubhghaill, W.R. Hagen, B.K. Keppler, K.-G. Lipponer and P.J. Sadler, J. Chem. Soc. Dalton Trans., (1994) 3305.
[18] J.D. Bell, R.E. Norman and P.J. Sadler, J. Inorg. Biochem., 31 (1987) 241.
[19] S.W.A. Bligh, H.A. Boyle, A.B. McEwen, P.J. Sadler and R.H. Woodham, Biochem. Pharmacol., 43 (1992) 137.
[20] J.D. Bell, G. Kubal, S. Radulovic, P.J. Sadler and A. Tucker, Analyst, 118 (1993) 241.
[21] N.A. Malik, G. Otiko, M.T. Razi and P.J. Sadler, Proc. Symp. on Bioinorganic Chemistry of Gold Coordination Compounds, SmithKline & French Labs., Philadelphia, PA, 1983, p. 82.

[22] A.A. Isab and P.J. Sadler, J. Chem. Soc. Dalton Trans., (1982) 135.
[23] M.T. Razi, G. Otiko and P.J. Sadler, ACS Symp. Ser., 209 (1983) 371.
[24] C.F. Shaw III, Comm. Inorg. Chem., 8 (1989) 233.
[25] P.J. Sadler and R.E. Sue, Met. Based Drugs, 1 (1994) 107.
[26] R.C. Elder, Z. Zhao, Y. Zhang, J.G. Dorsey, E.V. Hess and K. Tepperman, J. Rheumatol., 20 (1993) 268.
[27] R.C. Elder, W.B. Jones, Z. Zhao, J.G. Dorsey and K. Tepperman, Met. Based Drugs, 1 (1994) 363.
[28] G.G. Graham, G.D. Champion and J.B. Ziegler, Met. Based Drugs, 1 (1994) 395.
[29] G.G. Graham, J.R. Bales, M.C. Grootveld and P.J. Sadler, J. Inorg. Biochem., 25 (1985) 163.
[30] S.J. Berners-Price and P.J. Sadler, Struct. Bond., 70 (1988) 27.
[31] S.J. Berners-Price, C.K. Mirabelli, R.K. Johnson, M.R. Mattern, F.L. McCabe, L.F. Faucette, C.-M. Sung, S.-M. Mong, P.J. Sadler and S.T. Crooke, Cancer Res., 46 (1986) 5486.
[32] S.J. Berners-Price, G.R. Girard, D.T. Hill, B.M. Sutton, P.S. Jarrett, L.F. Faucette, R.K. Johnson, C.K. Mirabelli and P.J. Sadler, J. Med. Chem., 33 (1990) 1386.
[33] S.J. Berners-Price, D.C. Collier, M.A. Mazid, P.J. Sadler, R.E. Sue and D. Wilkie, Met.-Based Drugs, 2 (1995) 111.
[34] S.J. Berners-Price, R.J. Bowen and P.J. Harvey, unpublished results, 1996.
[35] S.J. Berners-Price and P.J. Sadler, J. Inorg. Biochem., 31 (1987) 267.
[36] S.J. Berners-Price, P.S. Jarrett and P.J. Sadler, Inorg. Chem., 26 (1987) 3074.
[37] S.J. Berners-Price, C. Brevard, A. Pagelot and P.J. Sadler, Inorg. Chem., 24 (1985) 4278; S.J. Berners-Price, R.K. Johnson, A.J. Giovenella, L.F. Faucette, C.K. Mirabelli and P.J. Sadler, J. Inorg. Biochem., 33 (1988) 285.
[38] S.J. Berners-Price, P.J. Sadler and C. Brevard, Magn. Reson. Chem., 28 (1990) 145.
[39] S.J. Berners-Price, R.J. Bowen, P.J. Harvey, G.A. Koutsantonis and R.E. Sue, in preparation.
[40] D.J. Darensbourg, C.-S. Chao, J.H. Reibenspies and C.J. Bischoff, Inorg. Chem., 29 (1990) 2153.
[41] B. Mohr, E.E. Brooks, N. Rath and E. Deutsch, Inorg. Chem., 30 (1991) 4541.
[42] J.A. Davies and S. Dutremez, Coord. Chem. Rev., 114 (1992) 61; R. Gobetto, Mater. Chem. Phys., 29 (1991) 221.
[43] S.J. Berners-Price, L.A. Colquhoun, P.C. Healy, K.A. Byriel and J.V. Hanna, J. Chem. Soc. Dalton Trans., (1992) 3357.
[44] E.M. Menger and W.S. Veeman, J. Magn. Reson., 46 (1982) 257.
[45] D. Affandi, S.J. Berners-Price, Effendy, P.J. Harvey, P.C. Healy, B.E. Ruch and A.H. White, in preparation.
[46] D.P. Bancroft, C.A. Lepre and S.J. Lippard, J. Am. Chem. Soc., 112 (1990) 6860.
[47] I.M. Ismail, S.J.S. Kerrison and P.J. Sadler, J. Chem. Soc. Chem. Commun., (1980) 1261.
[48] I.M. Ismail, S.J.S. Kerrison and P.J. Sadler, Polyhedron, 1 (1982) 57.
[49] S.J. Berners-Price and P.W. Kuchel, J. Inorg. Biochem., 38 (1990) 327.
[50] K.J. Barnham, S.J. Berners-Price, Z. Guo, P. del S. Murdoch and P.J. Sadler, Proc. 7th Int. Symp. on Platinum and Other Metal Coordination Compounds in Cancer Chemotherapy, Plenum, New York, 1996.
[51] D.L. Rabenstein and S. Fan, Anal. Chem., 24 (1986) 3178.
[52] J. Stonehouse, G.L. Shaw, J. Keeler and E.D. Laue, J. Magn. Reson. A, 107 (1994) 178.
[53] K.J. Barnham, S.J. Berners-Price, U. Frey, T.A. Frenkiel and P.J. Sadler, Angew. Chem. Int. Edn. Engl., 34 (1995) 1874.
[54] F. Gonnet, J. Kozelka and J.-C. Chottard, Angew. Chem. Int. Edn. Engl., 31 (1992) 1483.
[55] S.J. Berners-Price, T.A. Frenkiel, U. Frey, J.D. Ranford and P.J. Sadler, J. Chem. Soc., Chem. Commun., (1992) 789.
[56] K.J. Barnham, U. Frey, P. del S. Murdoch, J.D. Ranford and P.J. Sadler, J. Am. Chem. Soc., 116 (1994) 11175.
[57] K.J. Barnham, M.I. Djuran, P. del S. Murdoch, J.D. Ranford and P.J. Sadler, Inorg. Chem., 35 (1996) 1065.
[58] K.J. Barnham, D.R. Newell and P.J. Sadler, unpublished results.
[59] C.M. Riley, L.A. Sternson, A.J. Repta and S.A. Slyter, Anal. Chem., 130 (1983) 203.
[60] R.E. Norman, J.D. Ranford and P.J. Sadler, Inorg. Chem., 31 (1992) 877.

[61] P. del S. Murdoch, J.D. Ranford, P.J. Sadler and S.J. Berners-Price, Inorg. Chem., 32 (1993) 2249.
[62] S.J. Berners-Price, U. Frey, J.D. Ranford and P.J. Sadler, J. Am. Chem. Soc., 115 (1993) 8649.
[63] S.J. Berners-Price, J.D. Ranford and P.J. Sadler, Inorg. Chem., 33 (1994) 5842.
[64] J. Laussac and B. Sarkar, Biochemistry, 23 (1984) 2832.
[65] P.J. Sadler, A. Tucker and J.H. Viles, Eur. J. Biochem., 220 (1994) 193.
[66] C.M. Perkins, N.J. Rose, B. Weinstein, R.E. Stenkamp, L.H. Jensen and L. Pickart, Inorg. Chim. Acta, 82 (1984) 93.
[67] S.U. Patel, P.J. Sadler, A. Tucker and J.H. Viles, J. Am. Chem. Soc., 115 (1993) 9285.
[68] J. Christodoulou, P.J. Sadler and A. Tucker, Eur. J. Biochem., 225 (1994) 363.
[69] D.C. Carter and J.X. Ho, Adv. Prot. Chem., 45 (1994) 153.
[70] S.D. Lewis, D.C. Misra and J.A. Shafer, Biochemistry, 19 (1980) 6129.
[71] J. Christodoulou, P.J. Sadler and A. Tucker, FEBS Lett., 376 (1995) 1.
[72] R.R. Crichton, Inorganic Biochemistry of Iron Metabolism, Ellis Horwood, Chichester, 1991.
[73] P. Aisen, A. Leiberman and J. Zweier, J. Biol. Chem., 253 (1978) 1930.
[74] W.R. Harris and V.L. Pecoraro, Biochemistry, 22 (1983) 292.
[75] W.R. Harris, Biochemistry, 22 (1983) 3920.
[76] W.R. Harris and J. Sheldon, Inorg. Chem., 29 (1990) 119.
[77] W.R. Harris, Y. Chen and K. Wein, Inorg. Chem., 33 (1994) 4991.
[78] I. Bertini, C. Luchinat and L. Messori, J. Am. Chem. Soc., 109 (1983) 1347.
[79] A. Butler and M.J. Danzitz, J. Am. Chem. Soc., 109 (1987) 1864.
[80] J. Aramini and H.J. Vogel, J. Am. Chem. Soc., 115 (1993) 245.
[81] W. Kiang, P.J. Sadler and D.G. Reid, Magn. Res. Chem., 31 (1993) S110.
[82] J.M. Aramini and H.J. Vogel, J. Am. Chem. Soc., 116 (1994) 1988.
[83] S.G. Ward and R.C. Taylor, in M.F. Gielen (ed.), Metal-Based Antitumour Drugs, Freund, London, 1988, p. 1.
[84] F. Kratz, M. Hartmann, B. Keppler and L. Messori, J. Biol. Chem., 269 (1994) 2581.
[85] G. Kubal, P.J. Sadler and A. Tucker, Eur. J. Biochem., 220 (1994) 781.
[86] G. Kubal, P.J. Sadler and A. Tucker, J. Am. Chem. Soc., 114 (1992) 1117.
[87] G. Kubal, A.B. Mason, S.U. Patel, P.J. Sadler and R.C. Woodworth, Biochemistry, 32 (1993) 3387.
[88] G. Kubal, A.B. Mason, P.J. Sadler, A. Tucker and R.C. Woodworth, Biochem. J., 285 (1992) 711.
[89] E.J. Beatty, M.C. Cox, T.A. Frenkiel, G. Kubal, A.B. Mason, P.J. Sadler and R.C. Woodworth, in P.H. Collery, N.A. Littlefield and J.C. Etienne (eds.), Metal Ions in Biology and Medicine, John Libby Eurotext, Paris, 1994, p. 315.
[90] A. Bax, R.H. Griffey and B.L. Hawkins, J. Magn. Reson., 55 (1983) 301.
[91] G. Otting and K. Wüthrich, J. Magn. Reson., 76 (1988) 569.
[92] S.C. Brown, P.L. Weber and L. Mueller, J. Magn. Reson., 77 (1988) 166.
[93] A.M. Gronenborn, A. Bax, P.T. Wingfield and G.M. Clore, FEBS Lett., 243 (1989) 93.